A Dendrochronological Investigation of Paraglacial Activity and Streamflow in the Vicinity of the Homathko Icefield, British Columbia Coast Mountains, Canada

by

Sarah J. Hart
B.Sc., Mount Allison University, 2007

A Thesis Submitted in Partial Fulfillment
of the Requirements for the Degree of

MASTER OF SCIENCE

in the Department of Geography

Supervisory Committee

A Dendrochronological Investigation of Paraglacial Activity and Streamflow in Vicinity of the Homathko Icefield, British Columbia Coast Mountains, Canada

by

Sarah J. Hart
B.Sc., Mount Allison University, 2007

Supervisory Committee:

Dr. Dan J. Smith, (Department of Geography)
Co-Supervisor

Dr. John J. Clague, (Department of Earth Sciences, Simon Fraser University)
Co-Supervisor

Dr. Dennis E. Jelinski (Department of Geography)
Departmental member

Dr. Terri Lacourse (Department of Geography)
Departmental member

Abstract

Supervisory Committee:

Dr. Dan J. Smith, (Department of Geography)
Co-Supervisor

Dr. John J. Clague, (Department of Earth Sciences, Simon Fraser University)
Co-Supervisor

Dr. Dennis E. Jelinski (Department of Geography)
Departmental member

Dr. Terri Lacourse (Department of Geography)
Departmental member

Moraine and glacier dams bordering the Homathko Icefield burst in the 1980s and 1990s, causing catastrophic downstream floods. The largest of the floods occurred in August 1997 and was caused by rapid breaching of the dam that impounds Queen Bess Lake, below Diadem Glacier. The outburst flood from the lake eroded the Holocene-age sediment fill in the valley below, exposing a series of subfossil forest layers separated by overbank floodplain sediments. A field investigation of the eroded valley fill in 2008 revealed multiple paraglacial valley-fill units, many of which are capped by *in situ* stumps and woody detritus. Dendrogeomorphic dating and stratigraphic evidence revealed six major sediment deposition events that coincide with regional, independently dated glacier episodes over the past 1200 years. Construction of tree-ring chronologies for the study area also allowed for the examination of the relationship between radial tree growth and hydroclimate. Dendroclimatological and dendrohydrological techniques were used to reconstruct summer stream discharge of nearby Chilko River. An Engelmann spruce tree-ring chronology provided a proxy for mean summer discharge of Chilko River for the period 1775-2007. This record is the first to be developed from tree-ring

data for a river draining a glacierized watershed in the British Columbia Coast Mountains. This proxy record provides insights into streamflow variability of a typical Coast Mountains river over the past 232 years and confirms the long-term influence of the Pacific Decadal Oscillation and El Niño-Southern Oscillation teleconnections on hydroclimatic regimes in the region.

Table of Contents

List of Tables

List of Figures

Acknowledgements

My sincerest thanks are extended to my committee members: Dan Smith, John Clague, Terri Lacourse, and Dennis Jelinski. Their editorial comments and scientific insight were invaluable. I would like to thank my co-supervisors, Dan Smith and John Clague, for investing in me as a student and proving to be constant sources of encouragement. I would like to thank Dan for never shutting his office door, even after the fourth or fifth time I wheeled my chair into his office and startled him. I am also in debt to John for proving to be accessible whether on the mainland or in Argentina.

Thank you to my UVTRL lab mates; without you I never would have been able get through my field work or lab work. I would also like to acknowledge Kirsten Brown, Bethany Coulthard, Kate Johnson, and Kyla Patterson for their help in the field. Thanks to Sandy Allen, Lynn Koehler, and Sonya Larocque for the use of their chronologies in building my regional chronology and Kenna Wilkie for her subfossil chronologies. I'd also like to thank Colin Laroque, for his continued guidance in dendrochronology and in ways to appease Dan.

And finally, to my parents, for supporting me throughout my adventures in dendrochronology and trying to understand what exactly it is that I do and why I have to be all the way across the continent.

Chapter One: Introduction

1.1 Introduction

On August 12, 1997, the lower part of Diadem Glacier collapsed into Queen Bess Lake, a small lake adjacent to the Homathko Ice Field in the central Coast Mountains of British Columbia (Clague and Evans, 2000). About 6 x 10^6 m^3 of water drained from the lake and eroded valley-floor sediments over a distance of 8 km along the west fork of the Nostetuko River (Clague and Evans, 2000; Kershaw *et al*., 2005). A sequence of organic soils with *in situ* subfossil stumps and roots, separated by sheets of silt and sand, were exposed along the valley floor (Wilkie, 2006). The exposures and *in situ* stumps provided a unique opportunity to date, using dendrochronology, intervals of paraglacial fluvial aggradation in a typical river valley in the central Coast Mountains over the past 1200 years.

Aggradation occurs in response to changes in sediment load, discharge, and profile stability (Leopold and Bull, 1976). Sediment sequences resulting from aggradation can, in some instances, be important archives of climate (Vandenberghe, 2002). In proglacial mountain valleys, aggradation may occur during periods of glacier advance or retreat (Church and Ryder, 1972; Wilkie, 2006). A precise chronology for the onset of aggradation may be obtained by the dendrochronological dating of tree stumps rooted in peat or soil between clastic sediment units.

Most previous dendrochronological reconstructions of glacial history in the Coast Mountains have relied on dating trees damaged or killed by glaciers (Smith and Laroque,

1996; Allen and Smith, 2007; Jackson *et al*., 2008). This approach, however, provides an incomplete record, because Little Ice Age advances of the past several hundred years were the most extensive of the Holocene and destroyed or buried much of the evidence of earlier events (Koch *et al*., 2007; Menounos *et al.*, *in press*). Fluvial sequences downvalley of glacier forefields supplement and extend the direct glacial record; they provide a more complete, although less direct, record of climate and glacial activity (Wilkie, 2006).

Dendrochronology allows for climate reconstructions at annual resolution (Fritts, 1976). Proxy climate records are developed from trees by comparing widths of annual rings with time series of historical instrumental climate data. In coastal British Columbia, such analyses have provided proxy records of temperature and precipitation extending back over 500 years (Gedalof and Smith, 2001; Laroque, 2002; Larocque and Smith, 2005).

Previous research has shown that temperature and precipitation have significant effects on the discharge of streams in glaciated watersheds in British Columbia (Moore and Demuth, 2001). This association, along with the ability to reconstruct climate variables from tree rings, suggests that it may be possible to reconstruct annual or seasonal discharge of rivers in the Coast Mountains using climatically sensitive trees.

1.2 Research goals and objectives

Two goals underpinned my research. One was to examine the fluvial sedimentary response of Little Ice Age glacier activity on the west branch of the Nostetuko River.

Previous research in the valley indicated a process-response relationship between periods of floodplain aggradation and upstream glacier activity (Wilkie, 2006). The second goal was to explore the potential for reconstructing streamflow discharge from tree-ring records. Recent dendrohydrological research has demonstrated a relationship between Pacific ocean-atmosphere forcing and lake-level change in Alaska, showing that trees may archive hydrological information (Wiles *et al*., 2009). Related evidence that climate forcing associated with the Pacific Decadal Oscillation (PDO) and the El Niño-Southern Oscillation (ENSO) impacts streamflow dynamics within glacierized basins in British Columbia (Moore and Demuth, 2001), and prior dendroclimatic studies in the central Coast Mountains (Larocque and Smith, 2005) provided direction for my research.

Specific research objectives were to:

1. develop a local chronology for the dominant tree species at the study site,
2. use dendrogeomorphology and radiocarbon analysis to establish dates of floodplain stability and aggradation along the west branch of the Nostetuko River,
3. relate aggradation periods to existing records of glacier fluctuations during the Holocene in the Cordillera of northwestern North America,
4. document whether the annual radial growth characteristics of trees at the study site record a hydroclimatic signal, and
5. attempt to reconstruct the discharge of the Chilko River using dendrohydrology techniques.

1.3 Thesis format

The thesis consists of four chapters. The Introduction (Chapter One) is followed by two chapters that employ dendrochronology techniques to evaluate paleoenvironmental changes. Chapter Two describes paraglacial aggradation events in the west branch of the Nostetuko River valley. Chapter Three presents a dendroclimatic reconstruction of discharge in the Chilko River. These two chapters are formatted as manuscripts prepared for submission to refereed journals. Chapter Four summarizes the findings of the research, presents some concluding comments, and offers suggestions for further research.

References:

Allen, S.M. and Smith, D.J. 2007. Late Holocene glacial activity of Bridge Glacier, British Columbia Coast Mountains. Canadian Journal of Earth Sciences 44: 1753-1773.

Church, M. and Ryder, J.M. 1972. Paraglacial sedimentation: A consideration of fluvial processes conditioned by glaciation. Geological Society of America Bulletin 83: 3059-3072.

Clague, J.J. and Evans, S.G. 2000. A review of catastrophic drainage of moraine-dammed lakes in British Columbia. Quaternary Science Reviews 19: 1763-1783.

Fritts, H.C. 1976. Tree Rings and Climate. Academic Press, NY.

Gedalof, Z. and Smith, D.J. 2001. Interdecadal climate variability and regime-scale shifts in Pacific North America. Geophysical Research Letters 28: 1515-1518.

Jackson, S.I., Laxton, S.C. and Smith, D.J. 2008. Dendroglaciological evidence for Holocene glacial advances in the Todd Icefield area, Northern British Columbia Coast Mountains. Canadian Journal of Earth Sciences 45: 83-98.

Kershaw, J.A., Clague, J.J. and Evans, S.G. 2005. Geomorphic and sedimentological signature of a two-phase outburst flood from moraine-dammed Queen Bess Lake, British Columbia, Canada. Earth Surface Processes and Landforms 30: 1-25.

Koch, J., Clague, J.J. and Osborn, G.D. 2007. Glacier fluctuations during the past millennium in Garibaldi Provincial Park, southern Coast Mountains, British Columbia. Canadian Journal of Earth Sciences 44: 1215-1233.

Larocque, S.J. and Smith, D.J. 2003. Little Ice Age glacial activity in the Mt. Waddington area, British Columbia Coast Mountains, Canada. Canadian Journal of Earth Sciences 40: 1413-1436.

Larocque, S.J., and Smith, D.J. 2005. A dendroclimatological reconstruction of climate since AD 1700 in the Mt. Waddington area, British Columbia Coast Mountains, Canada. Dendrochronologia 22: 93-106.

Laroque, C.P. 2002. Dendroclimatic Response of High-Elevation Conifers, Vancouver Island, British Columbia. Unpublished Ph.D. dissertation. University of Victoria, Victoria, BC.

Leopold, L. and Bull, W.B. 1976. Base level, aggradation and grade. Proceedings of the American Philosophical Society 123: 168-202.

Menounos, B., Osborn, G., Clague, J., and Luckman, B. *in press*. Latest Pleistocene and Holocene glacier fluctuations in western Canada. Quaternary Science Reviews doi:10.1016/j.quascirev.2008.10.018.

Moore, R.D. and Demuth, M.N. 2001. Mass balance and streamflow variability at Place Glacier, Canada, in response to recent climate fluctuations. Hydrological Processes 15: 3473–3486.

Smith, D.J. and Laroque, C.P. 1996. Dendroglaciological dating of a Little Ice Age glacial advance at Moving Glacier, Vancouver Island, British Columbia. Géographie physique et Quaternaire 50: 47-55.

Vandenberghe, J. 1995. Timescales, climate and river development. Quaternary Science Reviews 14: 631-638.

Wiles, G.C., Krawiec, A.C., and D'Arrigo, R.D. 2009. A 265-year reconstruction of Lake Erie water levels based on North Pacific tree rings. Geophysical Research Letters 36(L05705): doi:10.1029/2009GL037164.

Wilkie, K.M.K. 2006. Fluvial response to Late Holocene glacier fluctuations in the Nostetuko River Valley, Southern Coast Mountains, British Columbia. Unpublished MSc thesis. Simon Fraser University, Burnaby, BC.

Chapter 2: A dendrogeomorphic reconstruction of Little Ice Age paraglacial activity in the vicinity of the Homathko Icefield, British Columbia Coast Mountains, Canada

Abstract

Moraine and glacier dams bordering the Homathko Icefield in the central British Columbia Coast Mountains failed in the 1980s and 1990s, causing catastrophic downstream floods. The largest of the floods occurred in August 1997 and was caused by overtopping and rapid breaching of the dam that impounds Queen Bess Lake, which borders Diadem Glacier. The floodwaters from Queen Bess Lake eroded Holocene-age sedimentary deposits along the west fork of Nostetuko River and caused a steep rise in the hydrograph of Homathko River at the head of Bute Inlet, approximately 115 km downstream. A field investigation of the eroded valley fill in 2008 revealed multiple paraglacial valley-fill units, many of which are capped by *in situ* stumps and woody detritus. Dendrogeomophological field techniques were employed to develop a chronology for the buried forests. To enable calendric dating a regional tree-ring chronology spanning the interval from AD 1572 to 2007 was constructed from living subalpine fir (*Abies lasiocarpa*) trees from seven sites in the southern Coast Mountains. In cases where subfossil stumps and boles predated the regional chronology, relative kill dates constrained by radiocarbon ages were assigned to floating chronologies. By combining these dendrogeomorphological dating methods, six floodplain aggradation episodes were identified within the past 1200 years. Comparison to local and regional

glacial histories suggests that these events reflect climate-induced Little Ice Age changes in local glacier cover.

Keywords – dendrogeomorphology, Homathko Icefield, Coast Mountains, paraglacial, tree-rings

2.1 Introduction

Glaciers throughout the British Columbia Coast Mountains are downwasting and undergoing rapid recession (Schiefer *et al*., 2007; Vanlooy and Forster, 2008). This deglacierization has been accompanied by an increase in the number and severity of floods and other catastrophic events in many mountain valleys (Evans and Clague, 1994). In the vicinity of the Homathko Icefield, failures of moraine and glacier dams during the 1980s and 1990s caused severe downstream flooding (Blown and Church, 1985; Clague and Evans, 2000; Kershaw *et al*., 2005). The largest of the floods occurred on August 12, 1997, and was caused by the collapse of the lower part of Diadem Glacier into proglacial Queen Bess Lake (Clague and Evans, 2000; Kershaw *et al*., 2005). The floodwaters from Queen Bess Lake eroded Holocene-age valley-fill deposits along the west fork of the Nostetuko River, exposing a series of sheets of silt and sand separated by organic horizons containing *in situ* tree stems and stumps. Wilkie (2006) and Wilkie and Clague (*in press*) interpreted the silt and sand sheets to be floodplain-wide aggradational units deposited in response to upvalley glacier fluctuations. Their interpretation and event chronology were based largely on radiocarbon ages obtained from the subfossil forest remains.

Sediment sequences resulting from aggradation are important climate archives (Vandenberghe, 1995). Floodplain aggradation and incision may occur in response to changes in glacier cover in glacierized watersheds (Church and Ryder, 1972; Church and Slaymaker, 1989). Dendrogeomorphological research methods are useful for dating

alternating periods of floodplain aggradation, stability, and erosion (Sigafoos, 1964; Nanson and Beach, 1977; Friedman *et al*., 2005; Mizugaki *et al*., 2006). Periods of floodplain stability can be determined by dating the oldest tree growing on a buried surface (Solomina, 2002; Stoffel and Bollschweiler, 2008). Once corrections are made for the ecesis period, a minimum period of floodplain stability can then be determined from the length of time recorded by the buried forest (Stoffel and Bollschweiler, 2008).

Dendrogeomorphological reconstructions provide insights into the activity of upstream glaciers on decadal to centennial timescales. Most prior dendroglaciological reconstructions in this region have relied on dating trees damaged or killed by glaciers (Smith and Laroque, 1996; Allen and Smith, 2007; Jackson *et al.,* 2008). This approach, however, provides an incomplete record, because Little Ice Age (LIA) advances of the past several hundred years destroyed or buried much of the evidence of earlier events. Fluvial sedimentary sequences outside glacier forefields provide an opportunity to supplement and extend the direct glacial record, because they provide a more complete, albeit less direct, record of climate and glacial activity (Wilkie, 2006).

The purpose of the research described in this paper was to develop an annually resolvable chronology of LIA floodplain aggradation events in the west fork of the Nostetuko River valley. These aggradation periods were then related to independently documented periods of LIA activity in the northwestern North America Cordillera.

2.2 Study Area

The study area is located in the middle reach of the west fork of the Nostetuko River (lat 51º 17 N, long 124º 30 W, ca. 1400 m asl), a glacier-fed stream found in the central Coast Mountains (Fig. 2.1). The west branch of the Nostetuko River originates at Diadem Glacier, an outlet glacier of the Homathko Icefield, which terminates in Queen Bess Lake below Mount Queen Bess (Fig. 2.1). The west branch flows into the main stem of the Nostetuko River 8 km below Queen Bess Lake. Nostetuko River, in turn, is a tributary of the Homathko River, which flows through the central Coast Mountains to tidewater at the head of Bute Inlet (Fig. 2.1).

The west branch of the Nostetuko River occupies a U-shaped valley in an area with more than 2000 m of vertical relief. The river flows through two rock canyons and across several alluvial reaches between Queen Bess Lake and the main stem of the river. The gradient of the river averages 3.8°, but ranges from 14° in the rock canyons to 0.5° in broad alluvial reaches (Kershaw, 2002). Lateral migration of the river is constrained by the steep valley slopes, rock canyons, and colluvial aprons and fans (Wilkie and Clague, *in press*).

Cold wet winters and warm dry summers characterize the study area. Climate normals (1961-1990) indicate the valley has an approximate annual average temperature of 0.7°C; mean monthly temperatures range from -8.8 °C to 9.7 ° (Wang *et al*., 2006). Average annual precipitation is about 1180 mm/yr, of which approximately 70-75% falls as snow from October through May.

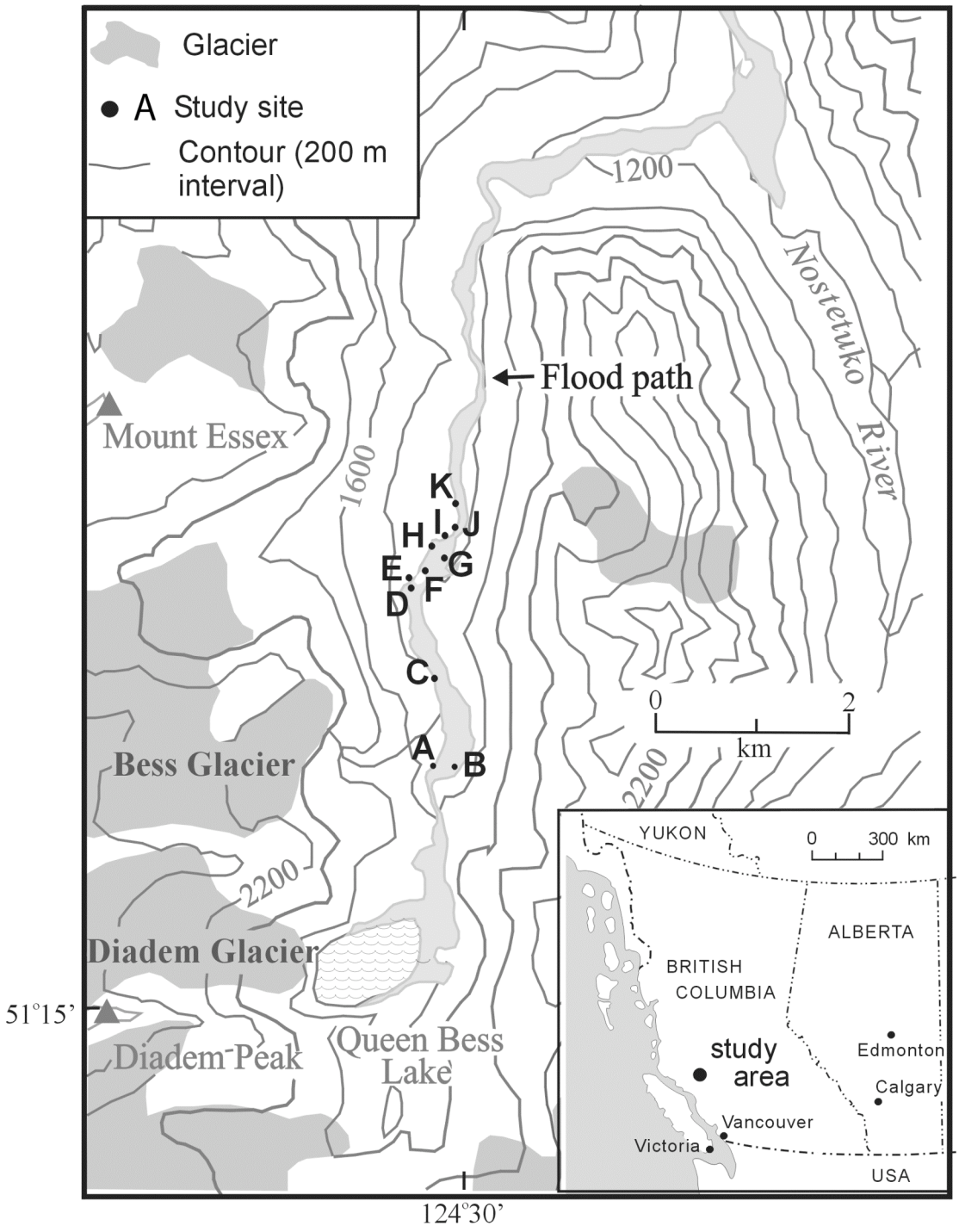

Figure 2.1: Locations of study sites within the west branch of the Nostetuko River valley (modified from Clague and Evans, 2000).

The valley lies within the Engelmann Spruce - Subalpine Fir (ESSF) biogeoclimatic zone (Meidinger and Pojar, 1991) and contains mixed stands of Engelmann spruce (*Picea engelmanni*), subalpine fir (*Abies lasiocarpa*), and whitebark pine (*Pinus albicaulis)*. Tree growth on steep valley walls is limited by snow avalanches. Mature stands of trees are restricted to the valley floor and to the surface of several large alluvial fans and colluvial aprons (Fig. 2.2). The upper limit of tree growth in the valley is ca. 1750 m asl.

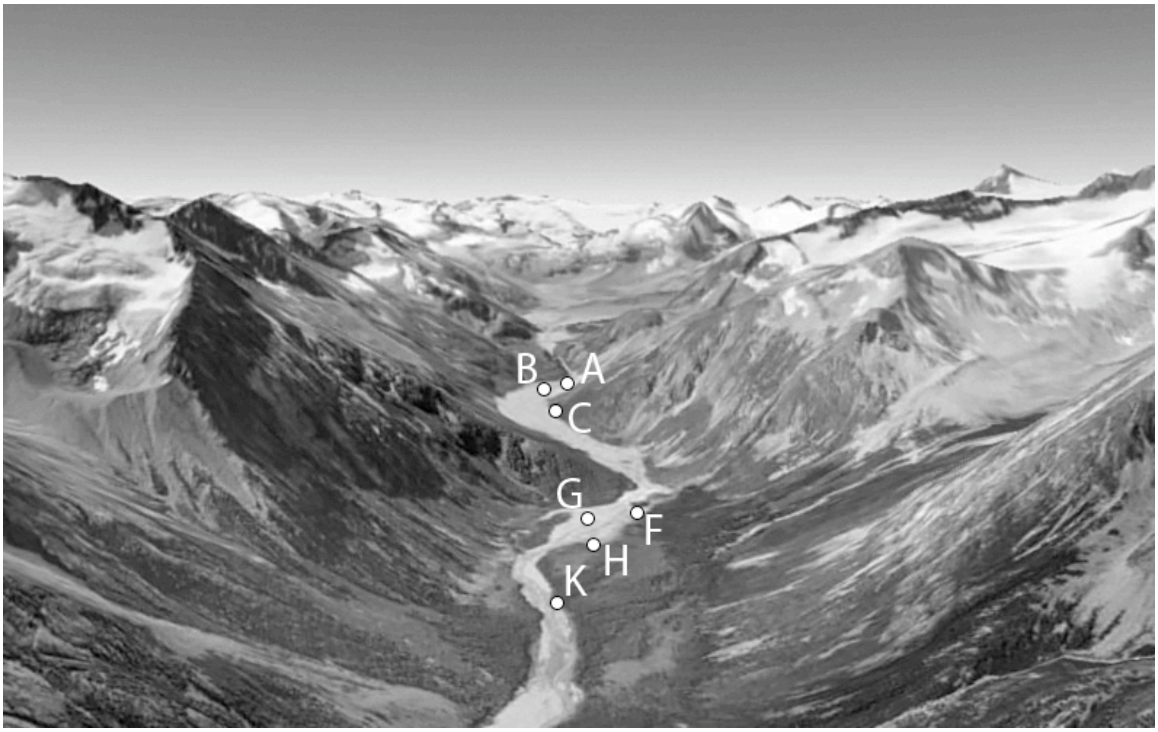

Figure 2.2: The west branch of the Nostetuko River valley. Note the high relief, extensive ice cover, and the broad river floodplain. Letters designate study sites described in text. (Modified from Google Earth, 2009).

2.3 Previous Research

Kershaw (2002) and Wilkie (2006) described the valley-bottom, clastic sediments eroded by floodwaters in 1997. Their investigations provide insights into the paraglacial history archived within the valley-fill sediments.

The west fork of Nostetuko River emerges from a rock canyon 1.25 km below Queen Bess Lake and truncates a large moraine fan complex constructed by the southern lobe of Bess Glacier (*unofficial name*) (Site A, Fig. 2.1). A branch collected from the base of the fan yielded a radiocarbon age of 2790 ± 60 ^{14}C yr BP (Fig. 2.3; Wilkie and Clague, *in press)*, coincident with the regional Tiedemann glacier advance reported by Ryder and Thomson (1986). A tree stem, exposed ca. 10 m below the surface of the fan returned a radiocarbon age of 150 ± 50 ^{14}C yr BP (TO-8932; Table 2.1).

River bank exposures downvalley of the moraine fan contain *in situ* stumps and boles rooted in a series of buried soil horizons and peat layers up to about 4 m above present river level. In many cases, these organic layers are not continuous or differ in thickness due to periods of erosion (Wilkie and Clague, *in press*). The horizons record periods of floodplain stability and soil development that are separated by units of silt and sand up to 1 m thick deposited during aggradational episodes (Wilkie, 2006; Wilkie and Clague, *in press*).

Table 2.1: Radiocarbon ages obtained in the west branch of the Nostetuko Valley from previous studies.

Site no.	Radiocarbon lab no.[a]	Radiocarbon age (^{14}C yr BP)[b]	Calibrated age range (cal yr AD)[c]	Calibrated age range mid-point (cal yr AD)	Material[d]
A	TO-8932	150 ± 60	1663-1895; 1903-1953	1808 ± 145	outer rings of *in situ* stump
B	TO-8923	370 ± 50	1445-1637	1541 ± 96	*in situ* root (Kershaw 2005)
E	Beta-200727	520 ± 50	1303-1365, 1383-1453	1378 ± 75	outer rings of *in situ* stump (sample ID 08A038)
E	Beta-200728	940 ± 50	1018-1209	1114 ± 96	outer rings of *in situ* stump (sample ID 08A040, 08A041)
F	Beta-200733	600 ± 60	1284-1424	1354 ± 70	outer rings of *in situ* stump
G	Beta-200725	620 ± 50	1284-1410	1347 ± 63	*in situ* root
I	TO-8935	110 ± 60	1669-1780, 1789-1944, 1950-1954	1812 ± 143	*in situ* root
I	Beta-200731	1030 ± 50	892-1052, 1080-1153	1023 ± 131	outer rings of *in situ* stump
K	Beta-200732	1160 ± 50	718-743, 769-990	854 ± 136	outer rings of *in situ* stump

[a] Laboratories: Beta – Beta Analytic Inc.; TO – IsoTrace Laboratory (University of Toronto).
[b] Ages have been corrected for natural and sputtering fractionation to a base of $\delta^{13}C$=-25.0‰.
[c] Determined from atmospheric decadal set of Reimer et al. (2004) using the online programme Calib 5.0. The range represents the 95.4% confidence limits.
[d] All samples were collected by Wilkie (2005) unless otherwise noted.

Radiocarbon dating of the exhumed stumps suggests that valley-floor forests were repeatedly buried during the last half of the Holocene, beginning as early as 5810 ± 70 ^{14}C yr BP (Wilkie 2006). Wilkie and Clague (*in press*) interpret these burial events as responses to upvalley glacier advances during the Garibaldi phase (mid-Holocene), Tiedemann advance (ca. 3000 yr ago), the First Millennium AD advance (ca. 1500 yr ago), and repeatedly during the Little Ice Age of the past 1000 years.

2.4 Methods

In July 2008, I conducted fieldwork at nine sites where subfossil tree stumps and stems were exposed along a 3 km reach of the river (Fig. 2.1). Six of the study sites were previously described by Wilkie (2006) and Wilkie and Clague (*in press*); three sites have not been previously reported (Table 2.2).

Table 2.2: Locations of study sites in the west branch of the Nostetuko River valley bottom.

Site no.		Latitude (N)	Longitude (W)	Elevation (m asl)
This study	Wilkie and Clague (*in press*)			
A	1	51º 16.30’	124º 30.28’	1473
B	2	51º 16.19’	124º 30.31’	1493
C		51º 16.46’	124º 30.27’	1448
D	3	51º 17.18’	124º 30.53’	1390
E	4	51º 17.19’	124º 30.56’	1389
F	5	51º 17.22’	124º 30.48’	1389
G	6	51º 17.38’	124º 30.37’	1408
H		51º 17.26’	124º 30.50’	1387
I	7	51º 17.41’	124º 30.26’	1380
J		51º 17.43’	124º 30.21’	1383
K	9	51º 17.65’	124º 30.17’	1381

I collected cross-section samples from subfossil trees exposed in the riverbanks using a chain saw. The stratigraphic position of each sample was noted and its height above river level was determined using a tape measure. A perimeter age was assigned to each sample by either cross-dating to a living chronology or by linking a floating tree-ring chronology to a radiocarbon age assigned to a perimeter wood sample.

2.4.1 Living chronology

I established a living tree-ring chronology from 40 increment core samples (20 trees, 2 cores each) collected from a mature stand of subalpine fir trees (>300 years in age) found growing adjacent to the river on a low-angle valley-bottom alluvial fan. The cores were transported to the University of Victoria Tree-Ring Lab (UVTRL), where they were air-dried and then glued into slotted mounting boards. I subsequently sanded the cores to a 600 grit polish to enhance annual rings (Stokes and Smiley, 1964). I measured ring-widths of each sample to the nearest 0.01 mm along a single radius using WinDendro software and a high-resolution flatbed scanner (Guay *et al*., 1992). A Velmex stage equipped with a microscope and video display was used with the computer programme MeasureJ2X (VoorTech Consulting, 2009) to measure widths of exceptionally narrow rings.

I constructed the chronology by cross-dating the series using common marker years (Stokes and Smiley, 1964). The International Tree Ring Database (ITRDB) computer programme COFECHA was subsequently used to verify block correlations between each tree-ring series and the master chronology to ensure adequate cross-dating (Holmes *et al.*, 1986). COFECHA correlations were calculated using a 50-year segment

length lagged successively by 25 years at a one-tailed 99% confidence level (Grissino-Mayer, 2001). Cores that exhibited aberrant growth patterns and were not significantly correlated to the group were removed from the data set.

The living tree-ring chronology was strengthened and extended back in time by supplementing it with six cross-dated subalpine fir chronologies previously collected by the UVTRL in the region (Table 2.3, Appendix 1a). The regional chronology incorporates only tree-ring data collected within 95 km of the study site on the relatively dry leeward slopes of the Coast Mountains.

Table 2.3: Locations of chronologies used in developing a regional subalpine fir chronology for the central British Columbia Coast Mountains.

Site	Latitude (N)	Longitude (W)	Elevation (m asl)	Source
Hope Glacier	51º 31’	124º 52’	1920	Larocque (2003)
Escape Glacier	51º 37’	125º 07’	1760	Larocque (2003)
Liberty Glacier	51º 35’	124º 49’	1525	Larocque (2003)
Cathedral Glacier	51º 14’	124º 51’	1600	Larocque (2003)
Homathko Icefield	51° 17’	124° 30’	1390	This study
Bridge Glacier	50º 48’	123º 29’	1544	Allen (2006)
Manatee Glacier	50º 36’	123º 38’	1600	Koehler (2009)

I constructed dendroclimatological analyses on both the site and regional chronologies to assess whether climate was limiting subalpine fir radial growth. A bootstrapped response function was used to test the relationship between annual radial growth and mean monthly climate parameters recorded at the nearest climate station (Tatlayoko Lake; station 1088010, lat 51º 40 N, long 24º 24 W, 870 m asl; Biondi and Waikul, 2003). In addition, I performed a wavelet analysis using Torrence and Compo’s

interactive website[1], to reveal periodicities in the dataset reflective of long-term oscillations in climate associated with broad-scale climate phenomena such as the Pacific Decadal Oscillation (PDO) and the El Niño-Southern Oscillation (ENSO) (Larocque and Smith, 2005).

2.4.2 Subfossil dendrogeomorphology

Floating tree-ring series were constructed from the subfossil cross-sectional samples by measuring ring widths along at least two radii (Appendix 2). Care was taken to use paths with the maximum number of rings and to avoid areas with reaction wood. Companion series from each subfossil sample were cross-dated using CDendro 7.1 (Larsson, 2003).

Species-specific floating chronologies were built from subfossil samples rooted in the same organic layer. The species of each sample was determined using a simple visual identification key and a light microscope (Hoadley, 1990). Correlation coefficients for the floating chronologies were calculated as an average linear correlation between each series. This method was selected because it provides conservative estimates of the year-to-year agreement between members of the chronologies.

Attempts were first made to cross-date individual floating chronologies to the local and regional living chronologies. Where successful, this cross-dating provided absolute kill dates. Where this approach was unsuccessful, radiocarbon ages of sample perimeter rings were used to provide approximate age constraints for the burial event (e.g. Koch *et al*., 2007).

---

[1] http://paos.colorado.edu/research/wavelets/

2.5 Observations and Results

2.5.1 Tree-ring chronologies

The local living subalpine fir chronology contains 29 series from 18 trees and spans 279 years (1729 to 2007 AD; Table 2.4). The series intercorrelation value calculated using 50-year segments, lagged successively by 25 years is significant at the 99% confidence level (0.444, Table 2.4).

Table 2.4: Tree-ring chronology statistics.

Site	Interval	No. series	Average series intercorrelation[a]	Average mean sensitivity
Local	1792-2007	29	0.444	0.214
Regional	1572-2007	257	0.513	0.214

[a] Calculated using computer programme COFECHA; default setting of 50-year segments with a 25-year overlap.

The composite regional chronology contains over 250 series and extends the tree-ring record back to 1572 AD (Table 2.4). COFECHA revealed a high degree of agreement between series (Table 2.4). The chronology, however, loses significant sample depth before 1725 AD (Fig. 2.4). Statistics calculated on the regional and site chronologies indicate similar sensitivities and intercorrelation values (Table 2.4). A strong correlation ($r = 0.53$) between the two chronologies was found using CDendro after detrending both average raw ring-width series with a negative exponential curve (Larsson, 2003).

The regional chronology correlated positively with current July temperature ($r = 0.39$) and negatively with previous July temperature ($r = -0.28$) at the 95% confidence

level. Wavelet analysis highlighted a periodicity of about 25 years (Gaussian 2 base function with a 5% white noise reduction; Torrence and Compo, 1998), indicative of the influence of the PDO on the growth of subalpine fir in this region.

2.5.2 Subfossil samples

A total of 135 subfossil trees were sampled on the Nostetuko valley floor (Appendix 2). Most of the samples were found in growth position, rooted in organic layers abruptly overlain by thick aggradational layers of silt and sand. The samples were identified as Engelmann spruce, subalpine fir, or mountain hemlock (Appendix 2). When flooded, conifers characteristically undergo changes in ring-width pattern *(*Sigafoos, 1964; Friedman *et al.,* 2005; Mizugaki *et al.,* 2006) or produce adventitious roots (Kozlowski *et al*., 1991). None of the 135 trees sampled showed evidence of adventitious roots. Periods of suppressed radial growth, traumatic resin canals, and reaction wood were observed in some of the samples, but they were restricted to the end of the ring series. The absence of adventitious roots and suppression of growth at the end of the trees' lives are interpreted to mean that most aggradation events were fatal, a less common but still documented response (Strunk, 1989). I interpret the periods of abnormal ring growth to represent the beginning of the aggradation period.

2.5.3 Site A

Site A is the fluvially eroded face of the large moraine fan below Bess Glacier (Fig. 2.3; Table 2.2). A laterally continuous mat of stumps, boles, and branch fragments is exposed ca. 10 m below the surface the fan. The downvalley orientation and character of the

detrital wood indicate that it was killed and buried during an advance of Bess Glacier into the valley. The perimeter rings of a bole recovered from the site in 2004 yielded a radiocarbon age of 150 ± 60 ^{14}C yr BP (TO-8932; Table 2.1). When visited in 2008, further erosion and collapse of the face had exposed additional detrital wood.

Cross-sections were collected from nine subfossil subalpine fir samples found within the moraine face and on the talus below. The oldest sample contained 97 annual growth rings. No bark was present on the samples and some perimeter rings were assumed missing due to weathering.

Three of the nine samples cross-date to form a 76-year-long floating chronology (Float VII; Table 2.5). This chronology cross-dates to the regional chronology and suggests that in ca. 1807 AD Bess Glacier was advancing over a moraine surface likely first colonized by trees about 1731 AD (Fig. 2.4). Assuming a local ecesis interval of five years (Wilkie, 2006) and that the oldest tree sampled was the first colonizer of a recently deglaciated surface, we infer that Bess Glacier had retreated some distance upvalley by mid 1720s.

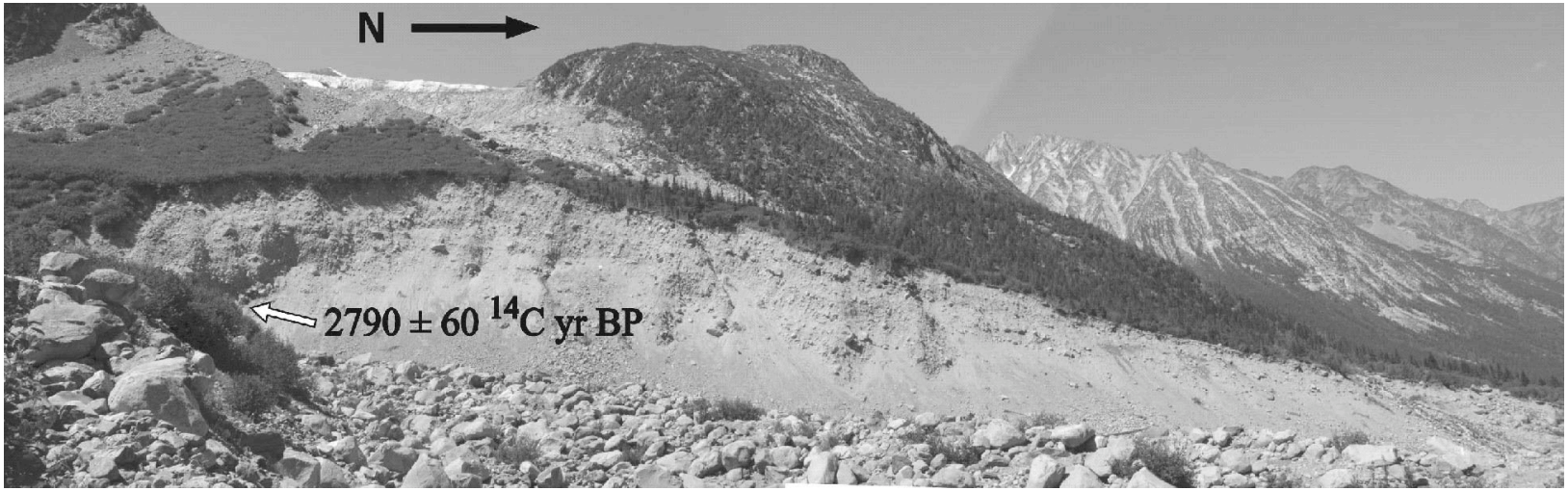

Figure 2.3: The eroded moraine fan complex at site A. Note the southern lobe of Bess Glacier, just visible above the moraine complex (modified from Wilkie and Clague *in press)*.

Table 2.5: Subfossil samples and floating chronologies developed in analyzing the paraglacial history of the west branch of the Nostetuko River valley bottom.

Subfossil series				Subfossil chronologies				
Sample ID[a]	Species[b]	Site	No. of rings	Name	Length (years)	Radiocarbon age (^{14}C yr BP)	No. of samples	r
08G003	saf	A	46	Float VII	76	150 ± 60	3	0.48
08G007	saf	A	76					
08G009	saf	A	60					
KW21	saf	B	102	Float VI	216	370 ± 50	3	0.49
08A044	saf	F	151					
08A045	saf	F	136					
08A043	saf	F	180	Float V	180	600 ± 60	2	0.31
08A048	saf	F	136					
KW15	saf	G	165	Float IV	245	620 ± 50	5	0.31
KW18	saf	G	92					
08A090	es	H	165					
08A093	saf	H	97					
08A094	saf	H	61					
08A040	saf	E	160	Float III	160	940 ± 50	2	0.35
08A039	saf	E	76					
08A108	saf	I	76	Float II	142	1030 ± 50	5	0.34
08A119	es	I	64					
08A121	saf	I	132					
08A091	saf	H	110					
08A092	es	H	135					
08A126	es	K	126	Float I	94	1160 ± 50	2	0.41
08A132	saf	J	78					
08A062	saf	H	152					
08A134	saf	C	137					
08A038	saf	E	152			520 ± 50		
08A108	saf	H	84			110 ± 60		

[a] 08A000 collected by the author; KW00 collected by Wilkie (2006).
[b] saf = subalpine fir; es = Engelmann spruce.

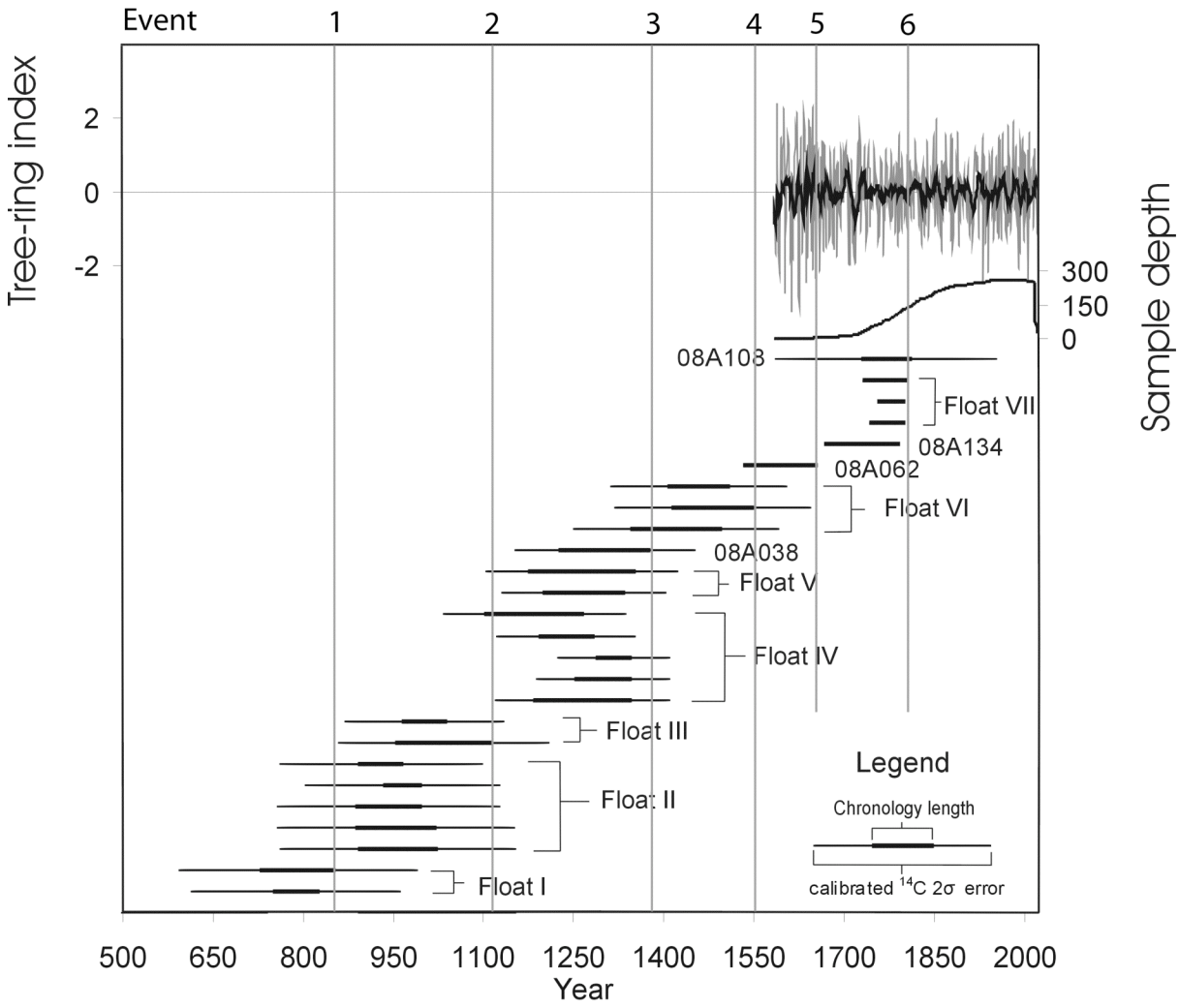

Figure 2.4: Tree-ring series constructed from sites in the Nostetuko River valley. The top gray line represents the regional subalpine fir COFECHA chronology; the black line is a five-year moving average. The sample depth of the regional chronology is plotted on the secondary y-axis. Subfossil floating chronologies are plotted below the regional chronology. Each line represents one sample; cross-dated samples are grouped with brackets. The six aggradation events are noted across the top x-axis.

2.5.4 Site B

Site B is the eroded face of a fluvial terrace on the east side of the river across from Site A (Fig. 2.1; Table 2.2). *In situ* roots and stumps are associated with a buried organic layer located about 3 m below the terrace surface. The outer rings of one of the stumps gave a radiocarbon age of 370 ± 50 ^{14}C yr BP (TO-8923; Table 2.1). Another stump, collected in 2004 by Wilkie (2006), was re-examined for this study. The rings of this stump form a 102-year-long series (Table 2.5). Correcting for ecesis, the minimum period of stability recorded by the organic layer at Site B is 107 years.

2.5.5 Site C

Site C is located on the west side of the valley, about 295 m north of Site A and adjacent to a small meltwater stream that flows from the southern lobe of Bess Glacier (Fig. 2.1). Two *in situ* rooted stumps were exposed in the bank of the stream, about 0.75 m below the surface. One of the two stumps (sample 08A134) was cross-dated to the regional tree-ring chronology and was 137 years old when it died in 1794 AD (Fig. 2.4). This finding suggests the site was stable from 1657 to 1794 AD, after which trees were killed and buried by sediment.

2.5.6 Sites D and E

Sites D and E are located on the west side of the river, 1.3 km downvalley from Site C (Fig 2.1). The sites are located along the upstream edge of a large treed valley-side alluvial fan. Erosion during the 1997 outburst flood scoured an elongate depression, exposing a thick sequence of alternating facies of stratified silt, sand, and peat. Site D is located at the southeast edge of the depression close to the forest. Site E is located at the

northwest edge of the abandoned floodway. The lowest exposed organic horizon at Site D was radiocarbon dated to 940 ± 50 C yr BP (Beta-200728; Table 2.1). The outer rings of a stump rooted in peat less than 1 m higher in the sequence yielded a radiocarbon age of 520 ± 50 ^{14}C yr BP (Beta-200727; Table 2.1). This finding and the presence of several other buried forest layers higher in the sequence suggest that trees repeatedly colonized overbank sediments on the valley floor at this site.

Forty-two cross-sections of stumps were collected at Sites D and E. Two *in situ* stumps of subalpine fir in the lowest organic horizon cross-date and form a 160-year-long floating chronology (Float III, Table 2.5). The trees were killed and buried by silt and sand in 940 ± 50 ^{14}C yr BP. It is inferred that this event was followed by a lengthy interval without significant aggradation, as a subalpine fir stump with 152 rings, slightly higher in the sequence, dates to 520 ± 50 ^{14}C yr BP (Beta-200727; Table 2.1).

2.5.7 Site F

Site F is located 100 m downvalley from Sites D and E at the north side of a forested bedrock knob (Fig. 2.2.). Sand separates two laterally extensive organic horizons, each of which contains *in situ* subalpine fir stumps. The lower organic horizon is at river level, about 3 m below the surface. Two cross-sections of these stumps cross-date to form a 180-year-long floating chronology (Float V; Table 2.5) with an outer perimeter wood age of 600 ± 60 ^{14}C yr BP (Beta-200733; Table 2.1).

The upper organic horizon is buried by ca. 1 m of fine sand (Fig. 2.5). Two cross-sections of stumps from this layer cross-date to form a 202-year-long floating chronology (Float VI; Table 5). This floating chronology cross-dates with the sample from site B; thus a perimeter date of 370 ± 50 ^{14}C yr BP was assigned to both (Table 5).

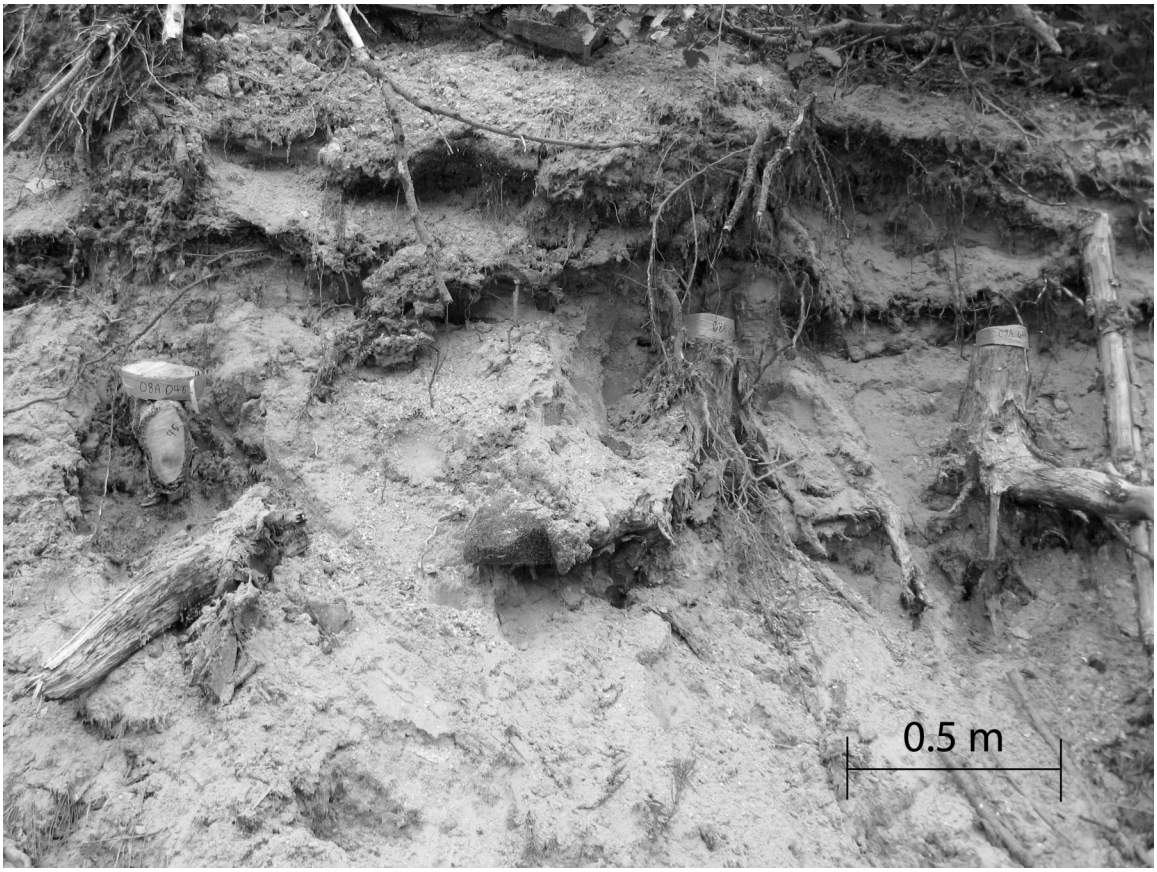

Figure 2.5: The top woody mat sampled at site F. Note the three *in situ* subfossil tree stumps in the photo and the massive layer of fine sand and silt that overlies them.

2.5.8 Site G

Site G is an exposure of silt and sand eroded by the 1997 outburst flood and located 315 m downvalley from Site F (Fig. 2.1). A buried peat layer less than 2 m below the surface contains *in situ* stumps. Cross-sections of two undated stumps collected by Wilkie (2006; KW15 and KW18) cross-date with radiocarbon-dated samples from Site H (Float IV, Table 2.5). This result indicates that the trees at Site G were killed in ca. 620 ± 50 ^{14}C yr BP (Beta-200725; Table 2.1), after a period of floodplain stability lasting at least 165 years.

2.5.9 Site H

Site H is a riverbank exposure 50 m downstream from site G at 1387 m asl (Figure 2.1; Table 2.2), along a side channel where exhumed stumps are exposed in the side of the riverbank (Figure 2.6).

Figure 2.6: The exposed subfossil wood at site H. The three stems in the foreground grew in the peat layer at the base of the section; the stems in the background are rooted 2.5 m below the top. Note the fine sand and silt that separate the two layers.

Two cross-sections of *in situ* stumps collected from the lowest organic horizon ca. 3.5 m below the surface cross-date to form a floating chronology. They also cross-date with samples from site I to form the 142-year-long floating chronology (Float II; Table 2.5) with a perimeter radiocarbon age of 1030 ± 50 ^{14}C yr BP (Beta-200731; Table 2.1). These results suggest that the trees growing at site H were killed and buried in 1030 ± 50

^{14}C yr BP following a period of floodplain stability that lasted at least 142 years (Table 2.5).

Six samples were collected from stumps found rooted within a second woody layer about 2.5 m below the surface. Three samples (two subalpine fir and one Engelmann spruce) cross-date with samples from site G (Float IV; Table 2.5). This finding suggests that these trees were killed 620 ± 50 ^{14}C yr BP after a period of floodplain stability lasting at least 245 years (Table 2.5).

A third organic layer is located within 1 m of the present-day ground surface. It contains snags that extend above ground level. Four stumps rooted in this horizon were sampled. Sample 08A062 cross-dates with the regional subalpine fir chronology and has a kill date of 1657 AD. This chronology extends back 152 years, indicating the floodplain was stable from 1505 to 1657 AD (Table 2.5).

2.5.10 Sites I and J

Site I is located 78 m downstream from Site H along the west bank of the river (Fig. 2.1). The site is actively eroding and significant slumping has exposed a 3 m sequence of bedded overbank silt and sand. Two prominent wood mats 1.5 and 3 m below the surface contain rooted stumps, and several thin organic horizons occur between the two mats.

Three samples from the lower wood mat cross-date to form a 142-year-long floating chronology (Float II; Table 2.5). The trees were killed and buried 1030 ± 50 ^{14}C yr BP (Beta-200731; Table 2.1) after a period of surface stability that lasted more than 76 years. Numerous sand layers with minor organic interbeds totaling 1.45 m in thickness

separate the lower horizon from the upper wood mat that was buried in 110 ± 60 ^{14}C yr BP (TO-8935; Table 2.1).

Site J is an exposure of flood-scoured overbank sediments adjacent to Site I (Fig. 2.1). Prominent organic layers occur at the base of the section and 1.5 m higher. Cross-sections were collected from several stumps in growth position, but only one of them (08A132) was successfully cross-dated to a sample at Site K with a perimeter age of 1160 ± 50 ^{14}C yr BP (Beta-200732; Table 2.5).

2.5.11 Site K

Site K is located 60 m downstream from Site J adjacent to the main river channel and is being actively eroded by the river (Fig. 2.2). A prominent non-erosive, thick peat layer, which gave a radiocarbon age of 1160 ± 50 ^{14}C yr BP (Beta-200732; Table 2.1), occurs at water level. Five cross-sections were collected from stumps rooted in the peat layer. One sample cross-dates with a 94-year floating chronology at Site J (Float I; Table 2.5). I infer that the floodplain was stable for at least 94 years, after which an episode of sediment aggradation buried and killed the trees at Sites I and J in ca. 1160 ± 50 ^{14}C yr BP.

2.6 Synthesis

The results of this investigation provide evidence for six major aggradation events during the past 1200 years (Fig. 2.4). The oldest event (no. 1) occurred 1160 ± 50 ^{14}C based on floating chronology I (Fig. 2.4). This chronology overlaps chronologies II and III in radiocarbon time, but none of the three chronologies cross-dates and the three organic layers differ significantly in character. This event appears to coincide in time

with a documented advance of Bridge Glacier, 90 km to the southeast, at 1190 ± 60 ^{14}C yr BP (Allen and Smith, 2007).

Event 2 is a valley-wide aggradation event that occurred at about 940 ± 50 ^{14}C yr BP. It is recorded at sites E, I, and H (Floats II and III; Fig. 2.7). Corresponding evidence for an interval of early LIA advance at this time comes from numerous sites in the northern (Haspel *et al*., 2005; Spooner *et al*., 2005) and southern Coast Mountains (Reyes and Clague, 2004; Allen and Smith, 2007; Koch *et al.,* 2007).

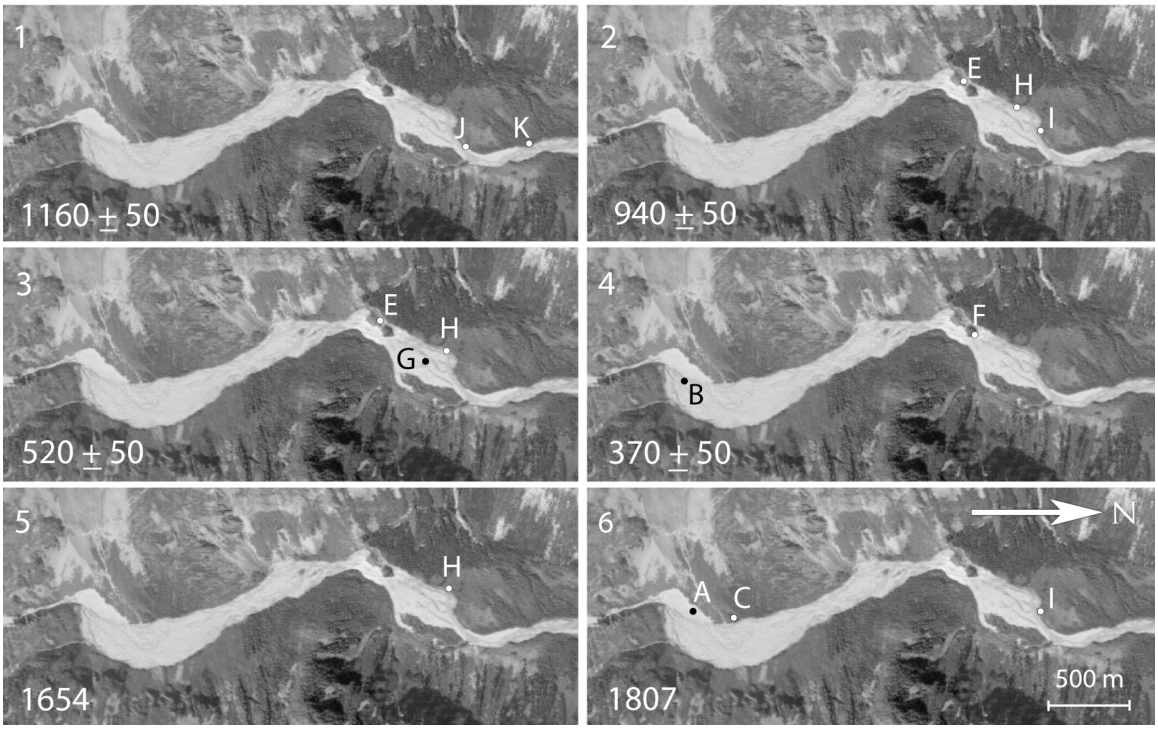

Figure 2.7: Inferred spatial extent of each of the six aggradation events documented in the west branch of the Nostetuko River valley. Sites with at least one sample dated to the event (number noted at top left, year at bottom left) are marked. (Modified from a 2005 Spot Image from Google Earth, 2009.).

Event 3 occurred in the late 14th century (600 ± 60 ^{14}C yr BP) and is recorded by an aggradation event at sites E, G, and H (Floats V and IV; Fig. 2.7). This time period is

widely recognized as an interval when glaciers were advancing throughout the southern Coast Mountains (Ryder and Thomson, 1986; Larocque and Smith, 2003; Lewis and Smith, 2004; Allen and Smith, 2007; Koch *et al*., 2007).

Event 4 is an aggradational episode ca. 370 ± 50 ^{14}C yr BP (Float VI, Fig. 2.3). Evidence for this event was found at Sites E, H, and I (Fig. 2.7). Glacier advances in the early to mid-1500s have been reported in the Mount Waddington area, 50 km to the northwest (Larocque and Smith, 2003).

Sediment deposited by Event 5 dates to 1657 AD and is documented at Site H (sample 08A062, Fig. 2.4). Evidence from Site C supports a major disturbance event ca. 1650 AD (sample 08A134, Fig. 2.7). Regional moraine stabilization in the mid to late 1660s (Larocque and Smith, 2003; Lewis and Smith, 2004) is consistent with the Event 5 paraglacial aggradation event.

Moraine construction at Site A in 1807 AD is contemporaneous with advances of other glaciers in the southern Coast Mountains during the LIA (Larocque and Smith, 2003; Menounos *et al.*, *in press*). Aggradation during Event 6, which occurred shortly after 1794 AD at Site C (sample 08A124), is consistent with a moraine-building episode at Site A at this time (Fig. 2.7).

2.7 Conclusions

A regional subalpine fir chronology was constructed for the period 1572-2007 AD from samples collected at seven sites in the southern Coast Mountains. This chronology was used to cross-date *in situ*, subfossilized trees bounded by layers of overbank sediments in the valley of the west fork of the Nostetuko River. Some of the exhumed forest horizons examined at the study site predate the regional chronology. In these cases,

floating chronologies were dated using radiocarbon ages on outer rings of subfossil trees in the valley. Using both methods, I documented and dated six, spatially extensive episodes of aggradation of the Nostetuko River floodplain during the past 1200 years. The six sedimentation events coincide with independently dated Neoglacial events in the Coast Mountains. They are assumed to reflect increased sediment delivery to the west fork of the Nostetuko River by Bess, Queen Bess, and other glaciers within the upper part of the watershed.

Most previous dendrochronological reconstructions of Holocene glacial history in the Canadian Cordillera have focused on trees that have been directly impacted by glaciers. This approach only captures some of the most recent glacier fluctuations, because the climactic advances of the late LIA buried or destroyed much of the evidence of earlier advances (e.g. Koch *et al*., 2007). Sediment supply to rivers draining glacierized catchments may change in response to an increase or decrease in ice cover. In some cases, the response is manifested in aggradation or incision of floodplains. As these environments lie outside LIA glacier limits, they may yield a more complete record of Holocene glacier activity than the evidence from glacier forefields themselves.

References

Allen, S.M. and Smith, D.J. 2007. Late Holocene glacial activity of Bridge Glacier, British Columbia Coast Mountains. Canadian Journal of Earth Sciences 44: 1753-1773.

Biondi, F. and Waikul, K. 2004. DENDROCLIM2002: A C++ program for statistical calibration of climate signals in tree-ring chronologies. Computers and Geosciences 30: 303-311.

Blown, I. and Church, M. 1985. Catastrophic lake drainage within the Homathko River basin, British Columbia. Canadian Geotechnical Journal 22: 551-563.

Church, M. and Ryder, J.M. 1972. Paraglacial sedimentation: A consideration of fluvial processes conditioned by glaciation. Geological Society of America Bulletin 83: 3059-3072.

Church, M. and Slaymaker, O. 1989. Holocene disequilibrium of sediment yield in British Columbia. Nature 327: 452–454.

Clague, J.J. and Evans, S.G. 2000. A review of catastrophic drainage of moraine-dammed lakes in British Columbia. Quaternary Science Reviews 19: 1763-1783.

Evans, S.G. and Clague, J.J. 1994. Recent climatic change and catastrophic geomorphic processes in mountain environments. Geomorphology 10: 107-128.

Friedman, J.M., Vincent, K.R., and Shafroth, P.B. 2005. Dating floodplain stability using tree-ring response to burial. Earth Surface Processes and Landforms 30: 1077-1091.

Grissino-Mayer, H.D. 2001. Evaluating cross-dating accuracy: A manual and tutorial for the computer program COFECHA. Tree-Ring Research 57: 205-221.

Guay, R., Gagnon, R., and Morin, H. 1992. A new automatic and interactive tree-ring measurement system based on a line scan camera. The Forestry Chronicle 38: 138-141.

Haspel, R., Osborn, J., and Spooner, I. 2005. Neoglacial deposits of Bear River Glacier, northern Coast Ranges, British Columbia. Annual Meeting, Western Division, Canadian Association of Geographers, University of Lethbridge, Lethbridge, AB.

Hoadley, R.B. 1990. Identifying Wood: Accurate Results with Simple Tools. The Taunton Press, Newtown, CT.

Holmes, R.L., Adams, R.K., and Fritts, H.C. 1986. Tree-ring chronologies of western North America: California, eastern Oregon and northern Great Basin, with procedures used in the chronology development work, including user manuals for computer programs COFECHA and ARSTAN. University of Arizona, Laboratory of Tree-Ring

Research, Chronology Series VI.

Jackson, S.I., Laxton, S.C., and Smith, D.J. 2008. Dendroglaciological evidence for Holocene glacial advances in the Todd Icefield area, northern British Columbia Coast Mountains. Canadian Journal of Earth Sciences 45: 83-98.

Kershaw, J.A. 2002. Formation and failure of moraine-dammed Queen Bess Lake, southern Coast Mountains, British Columbia. Unpublished M.Sc. thesis, Simon Fraser University, Burnaby, British Columbia.

Kershaw, J.A., Clague, J.J., and Evans, S.G. 2005. Geomorphic and sedimentological signature of a two-phase outburst flood from moraine-dammed Queen Bess Lake, British Columbia, Canada. Earth Surface Processes and Landforms 30: 1-25.

Koch, J., Clague, J.J., and Osborn, G.D. 2007. Glacier fluctuations during the past millennium in Garibaldi Provincial Park, southern Coast Mountains, British Columbia. Canadian Journal of Earth Sciences 44: 1215-1233.

Kozlowski, T.T. 1997. Responses of woody plants to flooding and salinity. Tree physiology monograph, No. 1 Heron Publishing, Victoria, British Columbia, Canada.

Larocque, S. 2003. Glacier and Climate Fluctuations During the Little Ice Age, Mt. Waddington Area, Southern Coast Mountains of British Columbia. Unpublished Ph.D. dissertation. University of Victoria, Victoria.

Larocque, S.J. and Smith, D.J. 2003. Little Ice Age glacial activity in the Mt. Waddington area, British Columbia Coast Mountains, Canada. Canadian Journal of Earth Sciences 40: 1413-1436.

Larocque, S.J. and Smith, D.J. 2005. A dendroclimatological reconstruction of climate since AD 1700 in the Mt. Waddington area, British Columbia Coast Mountains, Canada. Dendrochronologia 22: 93-106.

Larsson, L.A. 2003. CDendro - Cybis dendro Dating Program. Cybis Elektronik & Data AB, Saltsjöbaden, Sweden.

Lewis, D.H. and Smith, D.J. 2004. Little Ice Age glacial activity in Strathcona Provincial Park, Vancouver Island, British Columbia, Canada. Canadian Journal of Earth Sciences 41: 285-297.

Meidinger, D. and Pojar, J. 1991. Ecosystems of British Columbia. B.C. Ministry of Forests. Special Report Series No. 6. 330p.

Menounos, B., Osborn, G., Clague, J., and Luckman, B. *in press*. Latest Pleistocene and Holocene glacier fluctuations in western Canada. Quaternary Science Reviews doi:10.1016/j.quascirev.2008.10.018.

Mizugaki, S., Nakamura, F., and Araya, T. 2006. Using dendrogeomorphology and ^{137}Cs and ^{210}Pb radiochronology to estimate recent changes in sedimentation rates in Kushiro Mire, northern Japan, resulting from land use change and river channelization. Catena 3: 25-40.

Moore, R.D. and Demuth, M.N. 2001. Mass balance and streamflow variability at Place Glacier, Canada in response to recent climate fluctuations. Hydrological Processes 15: 3473-3486.

Nanson, G.C. and Beach, H.F. 1977. Forest succession and sedimentation on a meandering-river floodplain northeast British Columbia, Canada. Journal of Biogeography 4: 229-251.

Reimer, P.J., Baillie, M.G.L., Bayliss, A., Beck, J.W., Bertrand, C., Blackwell, P.G., Buck, C.E., Burr, G., Cutler, K.B., Damon, P.E., Edwards, R.L., Fairbanks, R.G., Friedrich, M., Guilderson, T.P., Hughen, K.A., Kromer, B., McCormac, F.G., Manning, S., Bronk Ramsey, C., Reimer, R.W., Remmele, S., Southon, J.R., Stuiver, M., Talamo, S., Taylor, F.W., van der Plicht, J., and Weyhenmeyer, C.E. 2004. IntCal04 terrestrial radiocarbon age calibration, 026 cal kyr BP. Radiocarbon 45: 1029-1058.

Reyes, A. and Clague, J.J. 2004. Stratigraphic evidence for multiple Holocene advances of Lillooet Glacier, southern Coast Mountains, British Columbia. Canadian Journal of Earth Sciences 41: 903-128.

Ryder, J.M. and Thomson, B. 1986. Neoglaciation in the southern Coast Mountains of British Columbia: chronology prior to the late Neoglacial maximum. Canadian Journal of Earth Sciences 23: 273-287.

Schiefer, E., Menounos, B., and Wheate, R. 2007. Recent volume loss of British Columbian glaciers, Canada. Geophysical Research Letters 34: doi:10.1029/2007GL030780, 2007.

Sigafoos, R.S. 1964. Botanical evidence of floods and flood-plain deposition. U.S. Geological Survey Professional Paper 485-A.

Smith, D.J. and Laroque, C.P. 1996. Dendroglaciological dating of a Little Ice Age glacial advance at Moving Glacier, Vancouver Island, British Columbia. Géographie physique et Quaternaire 50: 47-55.

Solomina, O.N. 2002. Dendrogeomorphology: Research requirements. Dendrochronologia 20: 233-245.

Spooner, I., Haspel, R., and Osborn, G.D. 2005. Holocene history of Bear River Glacier, northern Coast Ranges, British Columbia. *In* Water, Ice, Land, and Life: The Quaternary

Interface. Canadian Quaternary Association, University of Manitoba, Winnipeg, MB, p. A87.

Stoffel, M. and Bollschweiler, M. 2008. Tree-ring analysis in natural hazards research – An overview. Natural Hazards and Earth System Sciences 8: 187-202.

Stokes, M.A. and Smiley, T.L. 1964. An Introduction to Tree-Ring Dating. University of Chicago Press, Chicago, IL.

Strunk, H. 1989. Dendrogeomorphology of debris flows. Dendrochronologia **7:** 15–25.

Torrence, C. and Compo, G.C. 1998. A practical guide to wavelet analysis. Bulletin of the American Meteorological Society 79: 61-78.

Vandenberghe, J. 1995. Timescales, climate and river development. Quaternary Science Reviews 14: 631-638.

Vanlooy, J.A. and Forster, R.R. 2008. Glacial changes of five southwest British Columbia icefields, Canada, mid-1980s to 1999. Journal of Glaciology 54: 469-486.

VoorTech Consulting. 2008. MeasureJ2X [computer program]. Version 4.1.2. Holderness, NH.

Wang, T., Hamann, A., Spittlehouse, D., and Aitken, S N. 2006. Development of scale-free climate data for western Canada for use in resource management. International Journal of Climatology 26: 383-397.

Wilkie, K.M.K. 2006. Fluvial response to late Holocene glacier fluctuations in the Nostetuko River Valley, southern Coast Mountains, British Columbia. Unpublished M.Sc. thesis, Simon Fraser University, Burnaby, BC.

Wilkie, K.M.K. and Clague, J.J. *in press.* Fluvial response to Holocene glacier fluctuations in the Nostetuko River Valley, southern Coast Mountains, British Columbia. Geological Society of London Special Publication.

Chapter 3: A multi-species dendroclimatic reconstruction of streamflow in the Chilko River, British Columbia Coast Mountains, Canada

Abstract

In this study, I used dendroclimatological data to reconstruct the discharge history of the Chilko River, a typical river of those draining glacierized watersheds in the Coast Mountains of British Columbia. Ring-width records from Engelmann spruce (*Picea engelmanni*) and mountain hemlock (*Tsuga mertensiana*) trees were correlated to historical hydroclimate variables. Significant radial-growth relationships were revealed between temperature and spruce growth, as well as between precipitation and hemlock growth. These findings were used to reconstructed mean summer (June-July) discharge for the Chilko River from 1762 to 1999. This proxy record provided insights into streamflow variability of a typical Coast Mountains river over the past 240 years and confirms the long-term influence of the Pacific Decadal Oscillation and El Niño-Southern Oscillation teleconnections on hydroclimatic regimes in the region.

Keywords – British Columbia, Chilko River, dendrochronology, dendrohydrology, Engelmann spruce, streamflow reconstruction

3.1 Introduction

The Homathko Icefield extends over 2000 km^2 and is one of the largest icefields in the British Columbia Coast Mountains (Fig. 3.1). Outlet glaciers flowing from the icefield, like mountain glaciers elsewhere in the world, have thinned and retreated dramatically within the past few decades (Schiefer *et al.,* 2007; VanLooy and Forster, 2008). Meltwater streams issuing from these glaciers have significant hydrological influences on the downstream flow regimes of tributaries of the Fraser and Homathko rivers, which drain much of southern British Columbia (Fleming *et al.*, 2007). Given the environmental and economic importance of these rivers, increasing attention is being given to understanding how recent climate change is influencing their hydrology (Fleming and Clarke, 2003; Moore *et al.*, 2009).

The hydrology of glacier-fed rivers in this region is typically evaluated from the historic time-series of discharge maintained by the Water Survey of Canada (WSC, 2009). Although research has shown that the hydrologic regime of these rivers is climatically driven (Melack *et al*., 1997; Kiffney *et al*., 2002; Morrison *et al*., 2002), hydrometric records are of short duration and commonly contain data gaps (Fleming and Clarke, 2002). These deficiencies limit the temporal identification and understanding of possible relationships between low-frequency climate modes such as the Pacific Decadal Oscillation (PDO) and El Niño-Southern Oscillation (ENSO) on streamflow (Fleming *et al*., 2007). Shifting modes of large-scale ocean-climate circulation are known to influence glacier mass balance and streamflow in the mountains of Pacific North America (Moore and Demuth, 2001; Whitfield, 2001; Fleming *et al*., 2006), but longer-term records are required to fully assess the hydroclimatic impact of historic and ongoing climate change.

Tree-rings provide an opportunity to develop proxy records of streamflow (Stockton and Fritts, 1973; Meko *et al*., 2001; Case and MacDonald, 2003; Watson and Luckman, 2005). The objective of my research is to use climatically sensitive tree-ring records to reconstruct summer mean streamflow of the Chilko River, a major tributary of the Fraser River (Fig. 3.1). I also assess the influence of two Pacific climate modes (PDO and ENSO) on streamflow regimes over the past two centuries.

Previous prehistoric streamflow reconstructions in British Columbia have been developed from precipitation-sensitive tree species (Gedalof et al., 2004; Watson and Luckman, 2005). In this study mountain hemlock (*Tsuga mertensiana*), a species that typically shows a radial growth relationship to snow depth (Gedalof and Smith 2001a, Peterson and Peterson 2001, Larocque and Smith 2005) and Engelmann spruce (*Picea engelmanni* Parry), a species that characteristically shows a radial growth response to summer temperatures (Ettl and Peterson, 1995; Peterson *et al*., 2002; Wilson and Luckman, 2003), are used to reconstruct a proxy record of summer discharge for a snowpack-dominated basin within the Coast Mountains.

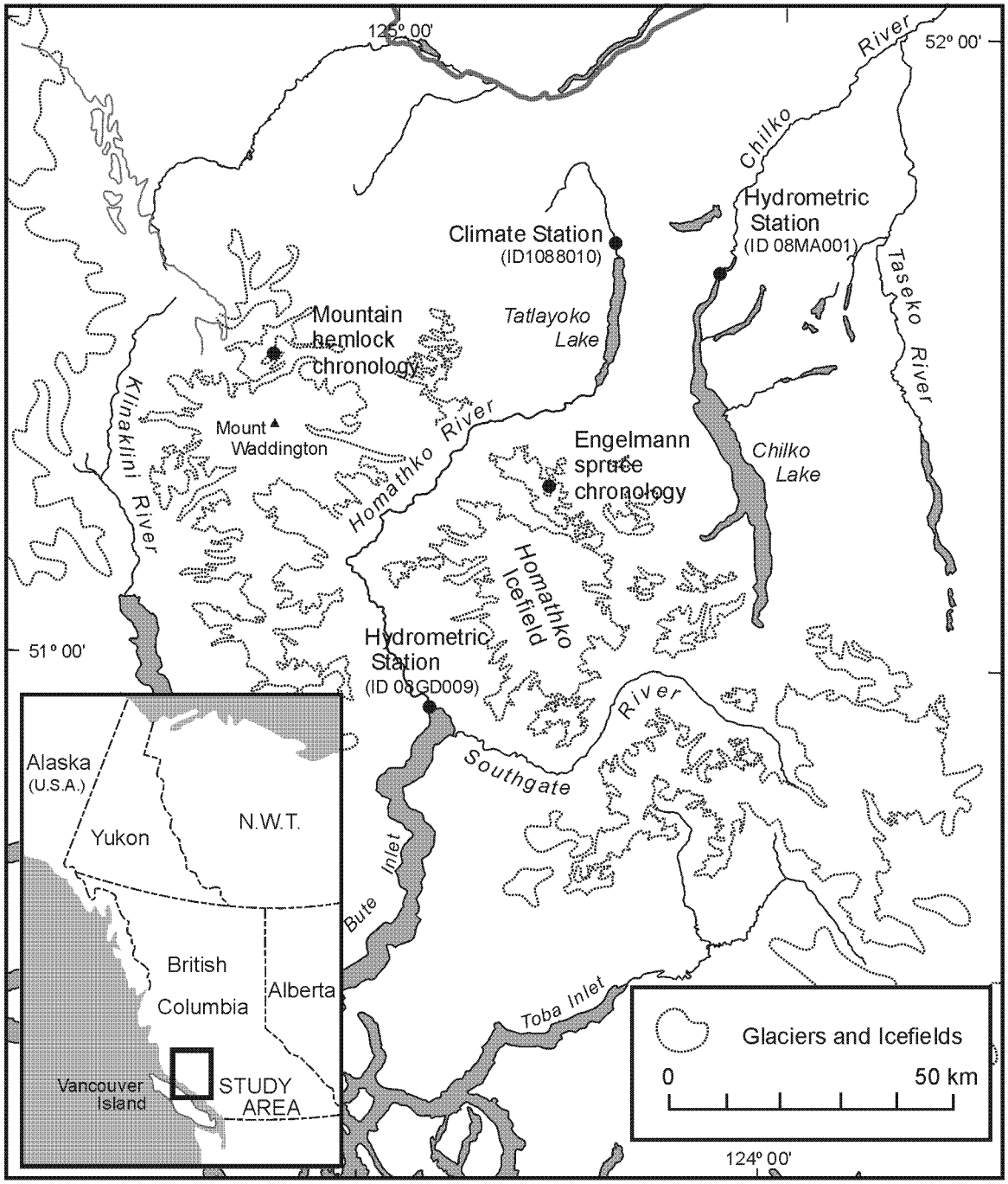

Fig. 3.1: Locations of climate station, tree ring chronologies, and hydrometric stations used in this study.

3.2 Background

Chilko River flows north from Chilko Lake to the Chilcotin River near the east margin of the southern Coast Mountains (Fig. 3.1). Chilcotin River, in turn, flows east to the Fraser River south of Williams Lake. Chilko River has been gauged at its outlet from Chilko Lake since 1928 (Station ID 08MA001, latitude 51°37.5' N, longitude 124°8.6' W; 2110 m asl). Mean monthly outflow from the lake has ranged from 4.41 m^3/s (February 1946) to 175 m^3/s (July 1991); the mean monthly average is 42.6 m^3/s over the period of record (WSC, 2009). A maximum instantaneous outflow discharge of 210 m^3/s was recorded on June 21, 1969 (WSC, 2009). Peak flows occur in late June or early July in response to seasonal melt of the snowpack in the Coast Mountains (Fig. 3.2; Whitefield, 2001). Streamflow is also augmented by glacier melt in the Homathko Icefield area in July and August (Moore *et al.*, 2009).

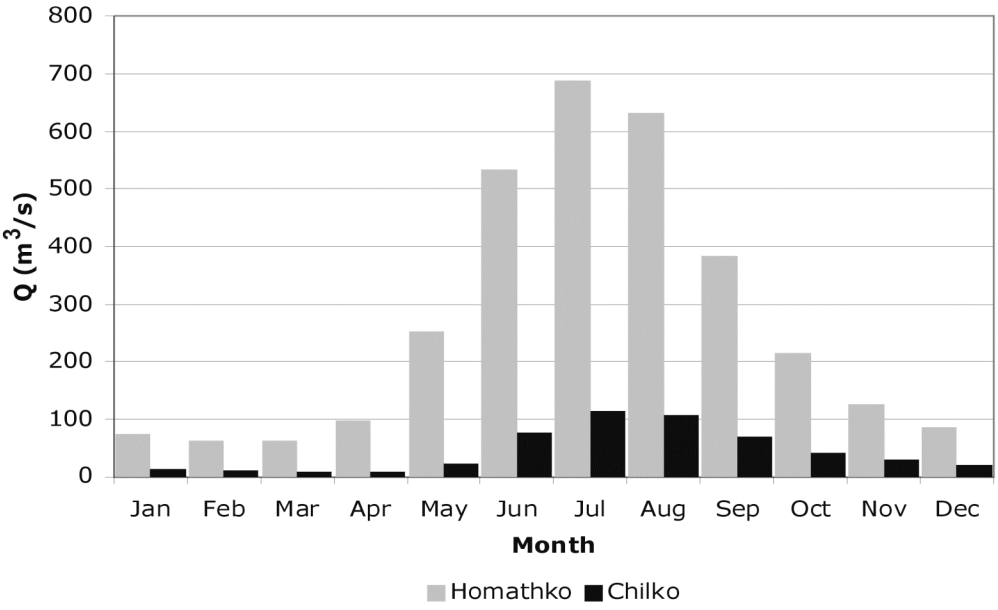

Fig. 3.2: Average monthly discharge of the Chilko and Homathko rivers. The disparity in discharge values, between the two rivers is in part due to the gauge location. Homathko River is gauged at its mouth and the Chilko River is gauged at its source.

Summer (June-July) discharge of the Chilko River has varied over the period of record (Fig. 3.3). Above-average flows in the early part of the record (1928-1940s) likely reflect warm summers. Above-average winter precipitation from 1940 until the early 1970s may be responsible for above-average mean flows during that period (Desloges and Gilbert, 1998). Decreased streamflow in the following two decades has been attributed to drier conditions and warmer temperatures (Whitfield, 2001).

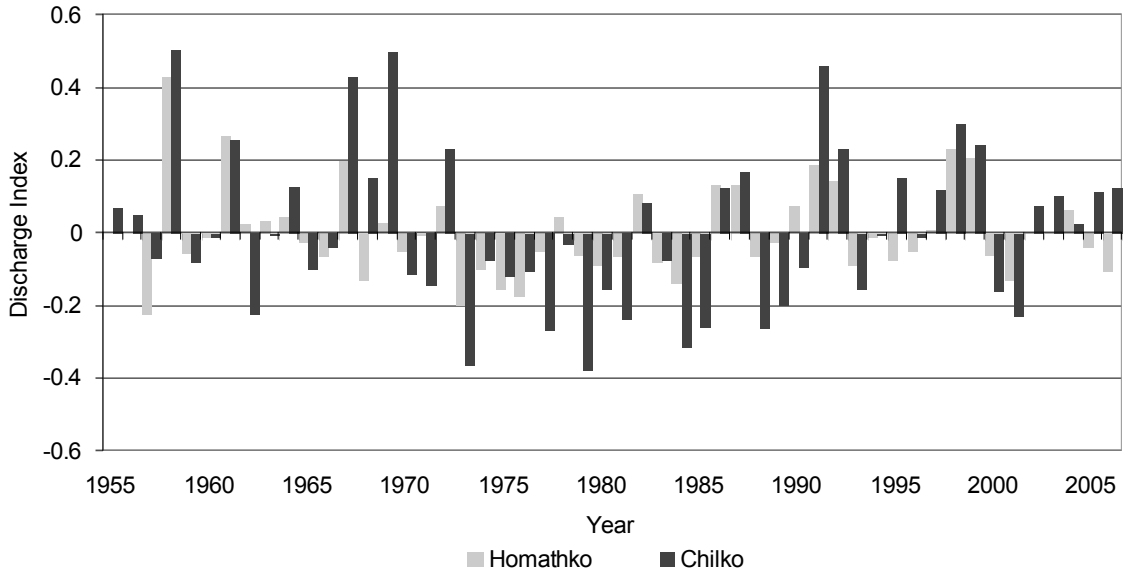

Fig. 3.3: Summer (June-July) mean discharge departures, Homathko and Chilko rivers. I calculated discharge index values by dividing the current year value by the historic average and subtracting one.

Comparison with climate data from the meteorological station at Tatlayoko Lake (Station ID 1088010, latitude 51º 40.2 N, longitude 124º 24.6 W; 870 m asl), 45 km north of the Chilko River gauging station, demonstrates that a significant part of this variability is a persistent hydrologic response to temperature variations. Average June-July temperature is significantly correlated to Chilko River mean summer streamflow (r =

0.518). Comparison with April-1 snowpack records from the nearest long-term snowpack record station, Tatlayoko Lake (Station ID 3A13, latitude 51º 36' N, longitude 124º 20' W, 1710 m asl), indicates that summer discharge is also related to the amount of winter snow accumulation. Chilko River mean summer streamflow is significantly correlated to April-1 snow water equivalent (SNWE) values ($r = 0.568$).

Chilko River streamflow is expected to show a systematic response to ENSO and PDO climate modes (Fleming and Quilty, 2006; Fleming *et al*., 2007). ENSO is a complex atmosphere-ocean interaction that causes cyclical warming and cooling of sea surface temperatures in the southern Pacific Ocean, with prominent global climatic teleconnections. In British Columbia, ENSO events over the past century have occurred, on average, every five to seven years, resulting in alternation of warm and cool climate states in Pacific North America (Ware, 2007). Sharp transitions from cool to warm states occur when positive phases of the PDO coincide with warm ENSO phases. The PDO is an atmosphere-ocean interaction that controls sea surface temperature in the North Pacific Ocean (Mantua and Hare, 2002). Warm phases of the PDO result in warmer temperatures and decreased winter precipitation in southern British Columbia; cool phases are accompanied by cooler temperatures and increased winter precipitation (Stahl *et al*., 2006). During the 20th Century, PDOs have switched states about every 15 to 25 years (Mantua and Hare, 2002), but proxy reconstructions back to 1600 AD suggest the presence of secondary PDO cycles with a periodicity ranging from 50 to 75 years (Gedalof and Smith, 2001b).

The interaction of these large-scale climate phenomena has significant effects in the western Canadian Cordillera (Moore and Demuth, 2001; Kiffney *et al*., 2002; Gobena

and Gan, 2006; Wang *et al*., 2006; Fleming *et al*., 2007). Unfortunately, our ability to understand and anticipate these interactions is limited by short instrumental records and poor resolution of most hydroclimate proxies (Walker and Pellatt, 2008). In contrast to most paleoenvironmental proxies, tree-ring records have annual resolution and offer the possibility of estimating streamflow prior to the period of direct monitoring (Case and MacDonald, 2003; Beriault and Sauchyn, 2006).

3.3 Study Area

The study area is located in the central British Columbia Coast Mountains, a highly glaciated region (Fig. 3.1). Climate within the central Coast Mountains is characterized by a shift from wet and maritime conditions on the southwest side of the range to a drier and more continental state on the northeast side. Climate normals (1971-2000) for the study site indicate an average annual air temperature of 0.9 ^{o}C and an average June-July temperature of 8.4 ^{o}C (Hamann and Wang, 2006). The annual total precipitation in the region averages 1180 mm/yr, of which approximately 70-75% falls as snow from October through May.

Much of this part of the Coast Mountains is drained by the Homathko River and its tributaries. The Homathko River is gauged at its mouth (Station ID 08GD009; latitude 51°25.3' N, longitude 124°30.4' W, 1550 m asl; WSC 2009). Its discharge is significantly correlated with that of the Chilko River ($r=0.710$; $p < 0.001$), which flows eastward into the Fraser River system. Peak flows of the Homathko and Chilko rivers in June-July are reflect contributions from snowmelt, augmented by some glacier melt (Fig. 3.2; Smith *et al*., 1987).

The study area is located within Engelmann Spruce - Subalpine Fir (ESSF) biogeoclimatic zone (Meidinger and Pojar 1991). Homogenous stands of mountain hemlock can be found on many slopes throughout the Homathko and Waddington ranges (Larocque and Smith 2005). Higher elevations are characterized by subalpine fir, except dry, disturbed sites, which are favoured by whitebark pine (*Pinus albicaulis*) (Meidinger and Pojar 1991). Two tree-ring sampling sites were selected within this study area.

3.3.1 Engelmann spruce study site

In July 2008, cores were collected from Engelmann spruce on a rocky well-drained alluvial fan adjacent to the west branch of the Nostetuko River at the edge of the Homathko Icefield (latitude 51°17.2' N, longitude 124°30.6'; 1390 m asl; Fig. 3.1; Appendix 1b). The west branch of the Nostetuko River is a glacier-fed stream in a valley that was affected by repeated catastrophic glacial outburst floods in the 20th Century (Blown and Church, 1985; Clague and Evans, 2000; Kershaw *et al*., 2005). Nostetuko River flows north and east toward the Chilcotin Plateau before swinging westward to join the Homathko River, which flows into Bute Inlet 45 km southwest of the field site.

The local forest on the alluvial fan is a mixed stand of Engelmann spruce, subalpine fir (*Abies lasiocarpa*), and whitebark pine (*Pinus albicaulis)*. Even-age spruce trees dominate and appear to have colonized the fan following its stabilization at the end of the Little Ice Age (Wilkie, 2006).

3.3.2 Mountain hemlock study site

The mountain hemlock chronology was established from tree cores collected in the summer of 2000 by the University of Victoria Tree-Ring Lab (UVTRL) at Oval

Glacier (historically known as Parallel Glacier; latitude 51°29.17' N, longitude 125°15.20'W; 1445 m asl; Fig. 3.1; Appendix 1c). Oval Glacier is a small valley glacier located on the north edge of the Waddington Range. The glacier has retreated over 800 m from its Little Ice Age maximum position and presently calves into proglacial Oval Lake (Larocque and Smith, 2003). Oval Lake drains into a small creek that flows into Scimitar Glacier. Meltwater from Scimitar Glacier flows into Scimitar Creek, which flows south and east before merging with Mosely Creek, a tributary of the Homathko River.

The steep mountain slopes above Oval Lake are characterized by a mixed stand of mountain hemlock and subalpine fir. Historic large snow avalanches on these slopes are recorded by the presence of treeless avalanche tracks and adjacent stands of youthful hemlock trees.

3.4 Methodology

3.4.1 Field collection

Standard dendrochronological techniques were used in collecting samples in the field (Stokes and Smiley, 1964). Trees representative of the forest were selected to create the longest ring-width records possible. Two increment cores were taken from twenty trees to ensure adequate replication. The cores were taken at breast height 180º from each other to account for differences in growth.

3.4.2 Chronology development

The cores were transported to the UVTRL where they were air-dried, glued into slotted mounting boards, and sanded to a 600-grit polish (Stokes and Smiley, 1964).

Ring-widths were measured to the nearest 0.01 mm along a single radius using WinDendro software and a high resolution flatbed scanner (Guay *et al*., 1992). For series with exceptionally narrow rings, a Velmex stage equipped with a microscope and video display was used in conjunction with MeasureJ2X (VoorTech Consulting, 2009) to measure the ring widths to the nearest 0.01 mm.

The ring-width series were visually cross-dated by comparing marker years between the series (Stokes and Smiley, 1964). The International Tree Ring Database (ITRDB) computer program COFECHA was employed to determine block correlations between each tree series and the master chronology (Holmes *et al*., 1986). COFECHA correlations were calculated using a 50-year segment length lagged successively by 25 years at a one-tailed 99% confidence level (Grissino-Meyer, 2000). Trees with growth patterns that were not significantly correlated to the group were removed from the data set.

Master tree-ring chronologies were calculated using the ITDRB program ARSTAN (Holmes *et al*., 1986). The program detrends each tree-ring series using a cubic smoothing spline to remove biological growth and other low-frequency trends. A spline rigidity of 32 years with a 50% frequency response level was chosen to generate the highest inter-series correlations and lowest standard deviations within the detrended series (Grissino-Mayer, 2001). Index values for residual growth were determined by dividing the actual ring width value by the value predicted from the spline. ARSTAN also uses a robust estimate of the mean to remove effects of endogenous and exogenous stand disturbances (Cook and Holmes, 1986). An autoregressive model was applied to

account for serial autocorrelation and provide a better estimate of the common signal (Cook and Holmes, 1986).

Expressed population signal (EPS) values were calculated for each chronology (Wigley *et al*., 1984). EPS is a statistic that expresses the degree to which the chronology signal is given when series are averaged. EPS values were calculated at 25-year moving periods for each chronology to quantify signal strength through time using computer programme COFECHA (Wilson and Luckman, 2003).

3.4.3 Climate and hydrometric data

Mean, maximum, and minimum monthly temperature and precipitation data for the closest meteorological station at Tatlayoko Lake were obtained from the Adjusted Homogenized Canada Climate Data website (AHCCD, 2009). April 1st snowpack data for Tatlayoko Lake were acquired from the B.C. Environment Historical Snow Survey Data website (B.C. Environment, 2009).

Mean, maximum, and minimum monthly streamflow data were obtained from the Water Survey of Canada website (WSC, 2009). Although the study site is located within the Homathko drainage basin, the discharge record for Homathko River spans only 49 years (1957-2006) and thus is inadequate for reconstruction. Consequently, data from the Chilko River station (1928-2006) were used. Missing values from this record were replaced with long-term monthly average values.

3.4.4 Reconstruction

Bootstrapped correlation and response function analyses were undertaken using the computer program DENDROCLIM2002 (Biondi and Waikul, 2004) to examine the

relationships between climate and annual radial growth (Appendix 3). Monthly mean discharge was compared with mean, minimum, and maximum monthly temperature and precipitation for the current and previous years. Data for the months of September to December of the current year were excluded from the analysis because most tree growth occurs before these months (Laroque and Smith, 2003). A simple Pearson's correlation was used to examine the relationship between April 1st snowpack and radial growth. Pearson's correlations were also calculated between discharge and tree-ring chronologies.

After determining the hydroclimatic relations with radial growth, a model of discharge was developed using multiple linear regression. Previous research has indicated that a linear relationship exists between tree rings and hydroclimatic variables, and improvements in explained variance are minimal when other statistical modeling techniques are used (Hughes, 2002). A forward stepwise linear regression was calibrated using the most recent 50% of the data. The ability of the model to fit the other 50% of the historic data was then checked using a Pearson's correlation. After verifying that the model was accurate, it was run through the period of overlap between the two chronologies.

3.4.5 Detecting modes of variability

Sea surface temperatures were used to determine if PDO and ENSO have influenced discharge over the past 150 years (D'Arrigo *et al*., 1999). The Hadley Centre's HADISST's global grided 1º latitude x 1º longitude mean monthly sea surface temperatures (SST) and sea-ice concentrations were correlated to the reconstructed

discharge index using the interactive KNMI climate explorer website[2] (van Oldenborgh and Burgers, 2005).

Wavelet analyses were employed to illustrate whether dominant modes of variability and localized variations in power exist within the Chilko River discharge record[3]. A Gaussian 2 function with a 5% white noise reduction, a method that has proved successful at discerning periodicity in the NINO3 SST index, was used as the base function (Torrence and Compo, 1998).

3.5 Results

3.5.1 Tree-ring chronologies

The Engelmann spruce master chronology spans 352 years (1656-2007 AD; Table 3.1). Prior to 1785, the chronology displays considerable annual variability due to limited sample depth (Table 3.2; Fig. 3.4). Anomalously narrow tree rings, which served to anchor the series, date to 1835, 1876, 1966, 1971, and 1979.

The mountain hemlock master chronology spans 237 years (1762-1999 AD; Table 3.1). The chronology shows considerable annual variability prior to 1845, which is attributed to low sample depth (Table 3.2; Fig. 3.4). Narrow marker years include 1872, 1887, 1894, 1911-13, 1916, 1921, 1976, and 1991.

[2] http://climexp.knmi.nl/
[3] http://paos.colorado.edu/research/wavelets/

Table 3.1: Tree-ring chronology statistics.

Site	Interval	No. series	Average series intercorrelation[a]	Average mean sensitivity
Engelmann spruce	1656-2007	38	0.468	0.174
Mountain hemlock	1762-1999	37	0.624	0.237

[a] Calculated using computer programme COFECHA; default setting of 50-year segments with a 25-year overlap.

Table 3.2: Expressed Population Values (EPS) for the mountain hemlock and Engelmann spruce chronologies as calculated by computer program ARSTAN.

Species	Year	Average no. cores	EPS value
Engelmann spruce	1760	12.7	0.68
	1785	24.7	0.89
	1810	33.0	0.92
	1835	36.4	0.91
	1860	37.0	0.91
	1885	37.4	0.91
	1910	37.9	0.92
	1935	38.0	0.94
	1960	38.0	0.95
Mountain hemlock	1820	6.0	0.77
	1845	8.7	0.80
	1870	13.0	0.92
	1895	21.1	0.94
	1920	29.2	0.95
	1945	34.9	0.95
	1970	37.0	0.97

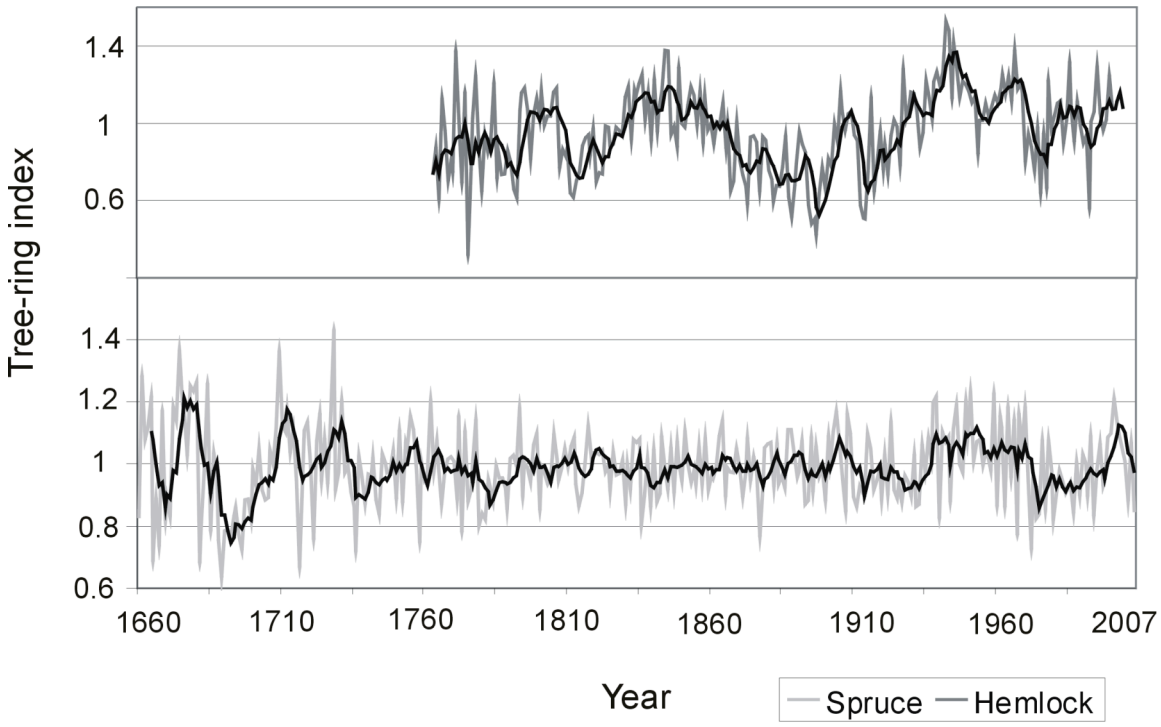

Figure 3.4: Tree-ring indices used in this analysis. The top time series is the mountain hemlock master chronology collected from Oval Glacier in 2000. The lower time series is the Engelmann spruce series collected from the west branch of the Nostetuko River in 2008. The dark lines are 5-year moving averages.

3.5.2 Dendroclimatic relationships

Correlation and response function tests show that both the Engelmann spruce and mountain hemlock chronologies are significantly correlated with air temperature (Fig. 3.5). The spruce chronology shows a significant negative relationship to the previous year's summer air temperature, a finding consistent with prior research in the Pacific Northwest (Ettl and Peterson, 1995; Peterson *et al.*, 2002). Similarly, the hemlock chronology shows a weak, but still significant negative correlation with previous summer temperature, a result consistent with previous tree-ring research in the area (Gedalof and Smith 2001b). Higher-than-average summer temperatures can cause increased

evapotranspiration and water loss, and decreased nutrient storage and foliage efficiency in trees. During warm summers, cone initiation may occur sooner and cone production may be greater (Ettl and Peterson, 1995; Klinka and Spelchtha, 1998; Zhang *et al*., 1999). These factors can result in decreased cambial activity and reduced radial growth in the following growth year (Rossi *et al*., 2006; Thibeault-Martel *et al*., 2008).

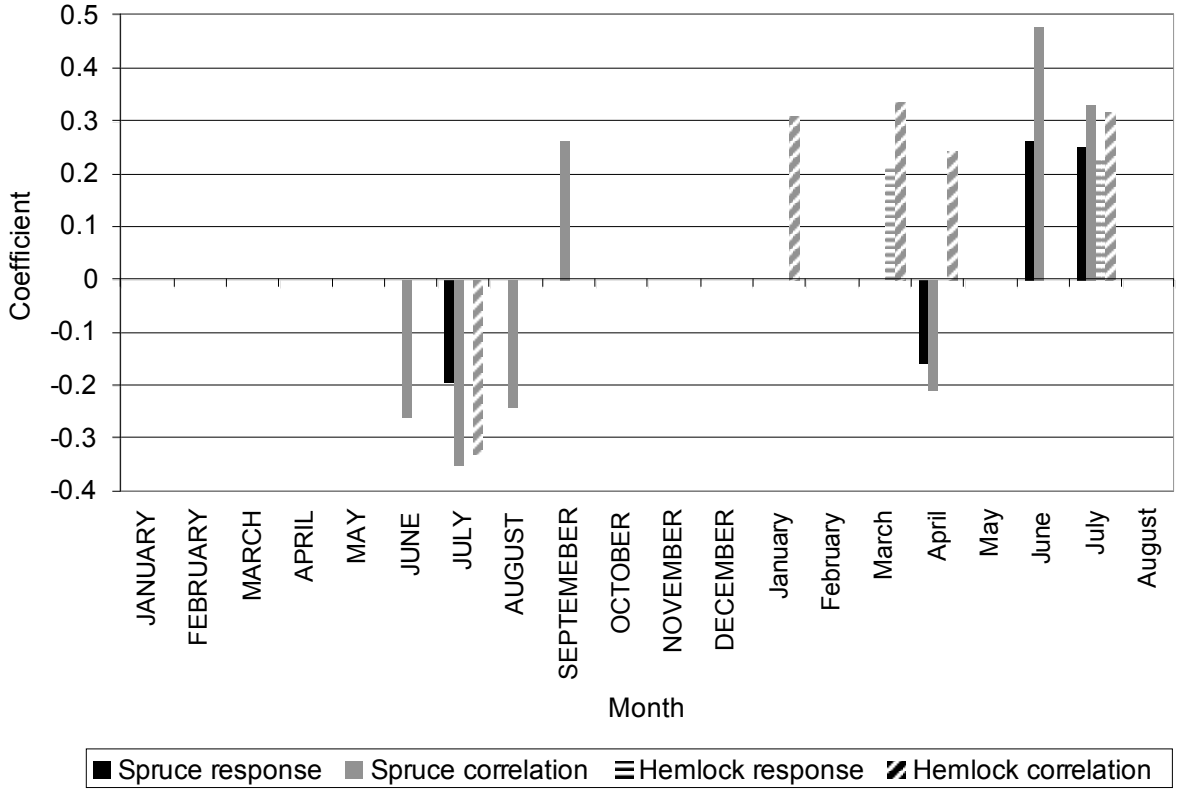

Figure 3.5: Response function and correlation coefficients for tree-ring series and mean temperature time series for each month from Tatlayoko Lake using DENDROCLIM2002. Months in block letters are from the previous year.

Mountain hemlock ring-width is also positively correlated to winter air temperature (Figure 3.5). Warmer-than-average winter temperatures likely enhance the survival of vegetative buds, leading to an increase in the photosynthetic potential of the

trees. This finding is consistent with other dendroclimatic research conducted in the British Columbia Coast Mountains (Larocque and Smith, 2005). The hemlock chronology was also found to be negatively correlated with April 1st snowpack records ($r = -0.452$). Photosynthesis and cambial production are limited by late-lying snow, thereby limiting the annual growth increment. Late-lying snow can reduce the effective length of the growing season by lowering soil temperature (Hansen-Bristow, 1986). Although little spring phenology data are available for mountain hemlock, this species probably behaves like subalpine fir in initiating leaf and shoot growth until after spring snowmelt (Peterson and Peterson, 2001).

The strongest temperature signal within both chronologies is a positive correlation to current summer temperatures (Fig. 3.1). Warmer temperatures during the summer months can result in earlier needle maturation and increased photosynthesis (Schmidt and Lotan, 1980). High early summer temperatures may also melt lingering snow, thereby increasing the length of the cambial growth season. This relationship is consistent with dendroclimatological relationships established with Engelmann spruce located in the Canadian Rocky Mountains (Luckman and Wilson, 2005) and interior British Columbia (Wilson and Luckman, 2003). Previous research has also identified positive correlations between hemlock and summer temperatures in the Pacific Northwest (Gedalof and Smith, 2001a; Peterson and Peterson, 2001; Larocque and Smith 2005).

3.5.3 Dendrohydrological relationships

Significant correlations between tree-ring growth and summer temperature and winter snowpack allowed for an examination of the relations between discharge and tree growth. A significant correlation exists between the spruce chronology and mean June

and July discharge (r = 0.454). Warmer summer temperatures drive snow melt (Whitefield, 2001). The amount of snow that is available for melt in summer is indicated by the mountain hemlock chronology. Because the hemlock chronology also contains a summer temperature signal, a partial correlation analysis was undertaken. The hemlock ring series and summer discharge were correlated while holding the spruce ring series constant. A significant negative correlation was identified between the hemlock chronology and mean summer discharge (r = - 0.371).

3.5.4 Dendrohydrological reconstructions

Stepwise multiple linear regression was used to model the relationship between mean summer discharge of the Chilko River and radial tree-ring growth for the calibration period 1965-1999 (Fig. 3.6). The model is significantly correlated to the historic streamflow data over both the calibration (r = 0.713) and verification (1928-1965; r = 0.527) periods (Table 3.3). Based on the strength of the relationship between tree growth and summer stream flow, a proxy summer discharge anomaly record for the Chilko River was constructed for the period 1762-1999 (Fig. 3.7). Over the instrumental period, the reconstruction appears to successfully model low-frequency variations and in general is more powerful at modeling high discharge values than low ones (Fig. 3.7). Anomalously low flows are inferred for the summers of 1780, 1783, 1835, 1973, 1979, and 1993; high flows are inferred for the summers of 1811, 1887, 1903, 1952, and 1969 (Fig. 3.7).

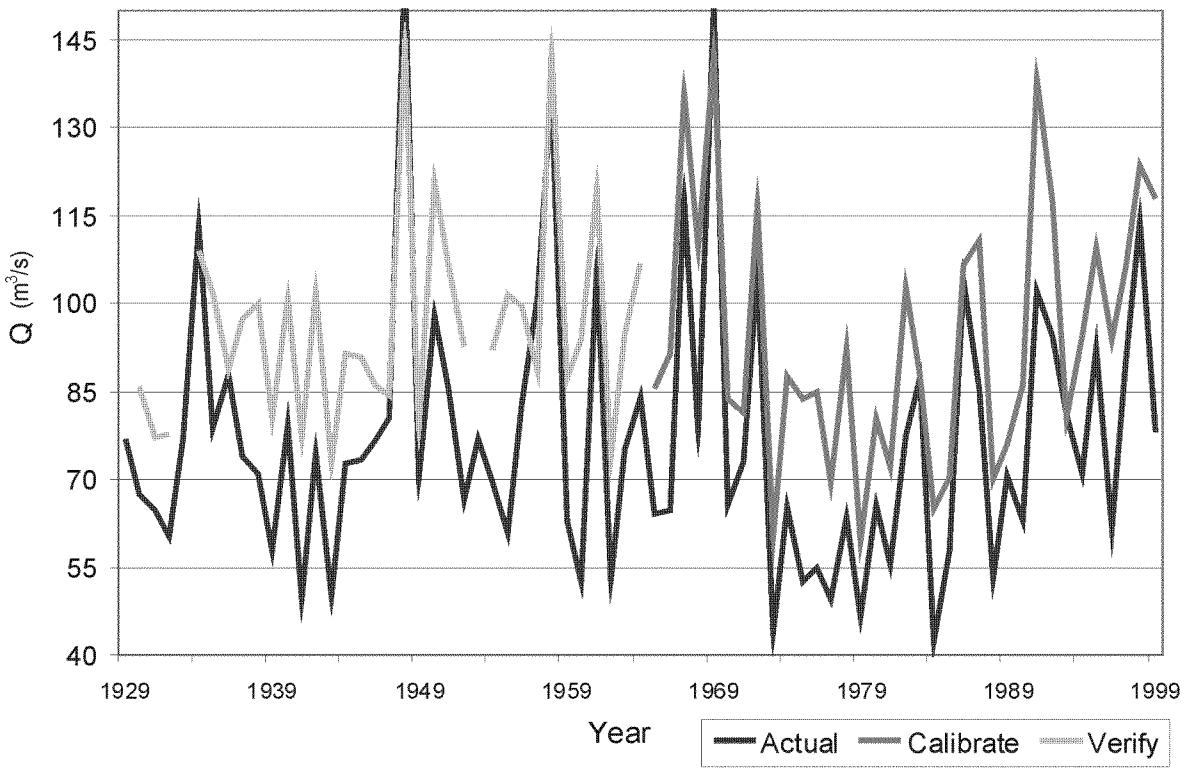

Fig. 3.6: Mean summer discharge model for the Chilko River based on linear relationships with the radial growth of Engelmann spruce and mountain hemlock.

Table 3.3: Model summaries for mean summer temperature and stream flow reconstructions using Engelmann spruce ring width as the predictor.

	Model[a]	Calibration correlation	Verification correlation	Total correlation
Mean summer stream flow	y = 42.13 + 120.60(es) – 64.31(mh)	0.713	0.527	0.634

a – es = Engelmann spruce; mh = mountain hemlock.
All correlations are significant at the 99% confidence level..

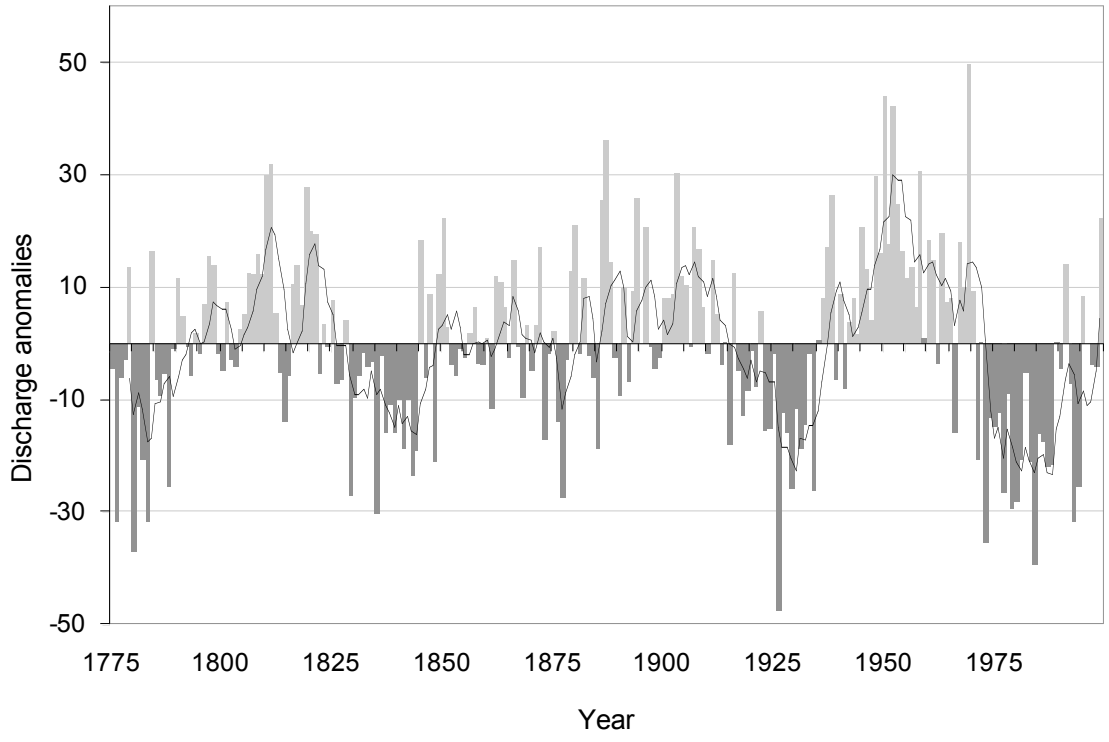

Fig. 3.7: Reconstructed discharge anomaly record for Chilko River. The solid line represents a 5-yr moving average.

3.5.5 Identifying modes of variability

Winter (Jan-April) sea surface temperatures (SST) in the northeast Pacific and South Pacific oceans correlate with the reconstructed discharge time series ($p<10\%$) over the period 1870-1999 (Fig. 3.8). The correlation between the reconstructed discharge time series and SST fields in the South Pacific is negative. This relationship is interpreted to be a response to ENSO phases that result in warmer-than-normal temperatures and slightly drier conditions in coastal British Columbia (Mantua *et al.*, 1997; Kiffney *et al.*, 2002).

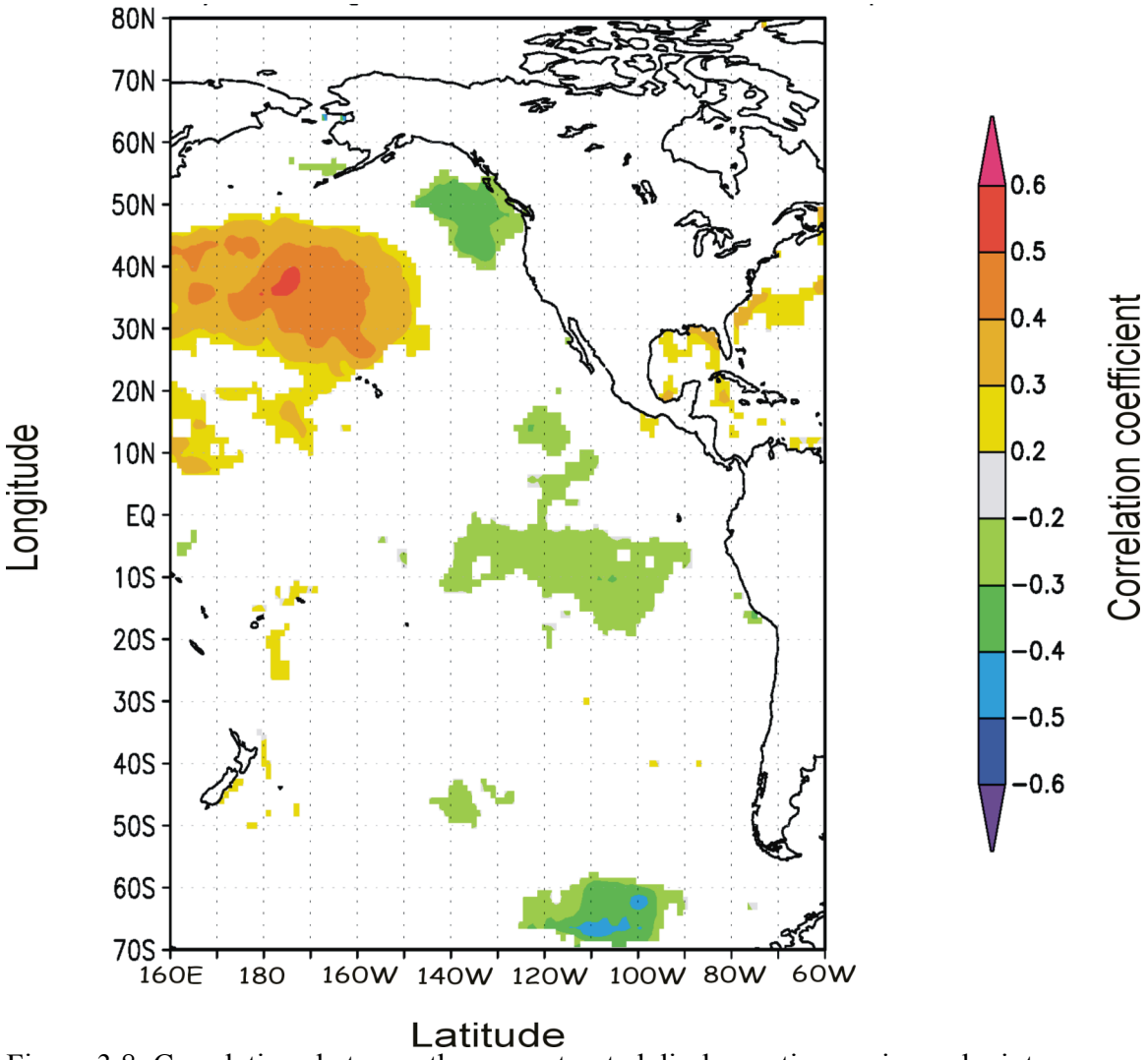

Figure 3.8: Correlations between the reconstructed discharge time series and winter sea surface temperature (Jan-April) using KNMI climate explorer.

Correlations with northeast Pacific Ocean SST suggest streamflow responds to persistent surface climate regimes accompanying the PDO (Fig. 3.9). In the negative phase of the PDO, sea surface temperatures in the northern Pacific Ocean are typically cool off the British Columbia coast and warm in the central North Pacific. During this phase of the PDO, watersheds in the British Columbia Coast Mountains are marked by conditions that are cooler and wetter than normal (Kiffney *et al*., 2002). A negative

correlation can be found between the reconstructed discharge and the winter PDO index ($r = -0.410$). Similarly a negative correlation exists between the winter PDO index and snowpack records. ($r = -0.515$). The positive correlation between the central North Pacific and discharge reflects the negative phase of the PDO, which results in increased snowfall and higher discharge in the region. The negative correlation identified between discharge and offshore winter SST reflects persistence of low SST into the summer months, causing lower-than-average summer temperatures and reduced snowmelt.

Wavelet analysis revealed dominant low and high-frequency modes of variability within the reconstructed 225-year streamflow record (Fig 3.9). Throughout this period, there is a persistent high-frequency variance in the seven-to-eight year band typical of ENSO. The analysis also indicates the presence of significant power in the ~ 50 year band, consistent with observed PDO behaviour. The streamflow reconstruction records a weakened PDO influence over the period 1850-1910 (Fig. 3.8), consistent with independent reconstructions of the PDO over that past two hundred years (Gedalof and Smith, 2001b; MacDonald and Case, 2005).

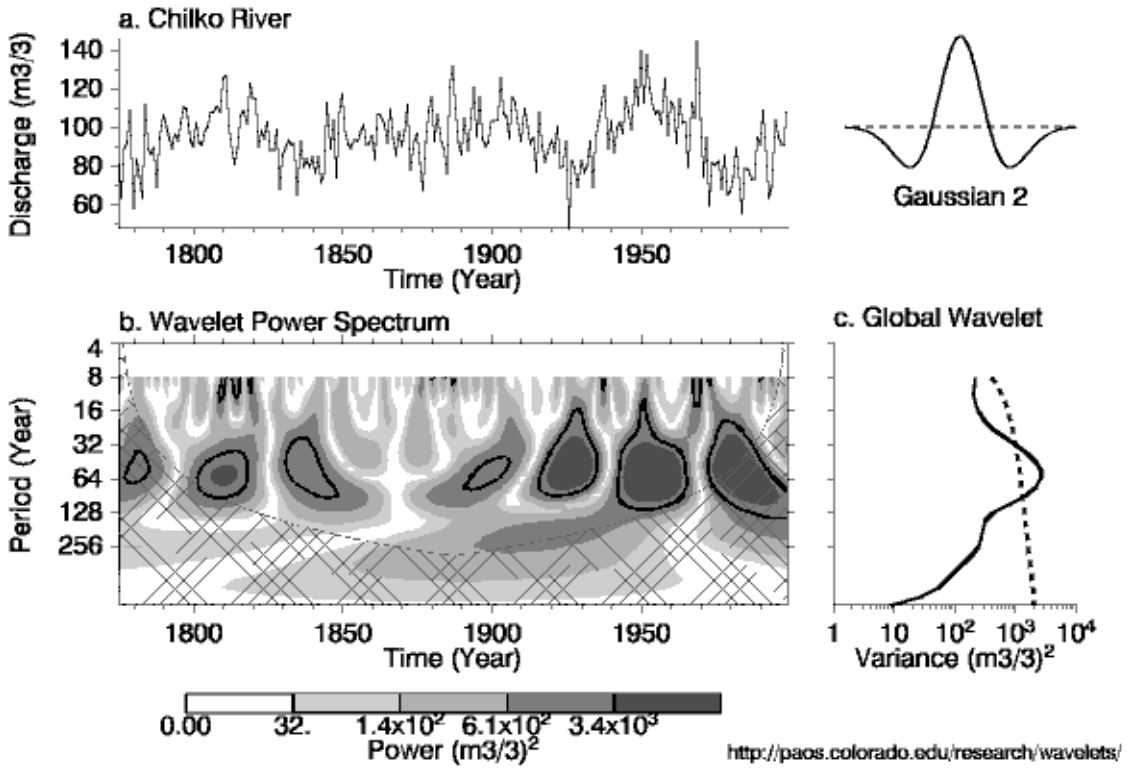

Fig. 3.9: (a) Proxy record of Chilko River discharge. (b) Wavelet power spectrum. The contour levels represent 75%, 50%, 25%, and 5% of wavelet power. The cross-hatched region represents the cone of influence where zero padding has reduced the variance. The black contours are the 5% significance levels, using a white-noise background spectrum. (c) Global wavelet spectrum (black line) and significance (dashed line), assuming the same background spectrum and significance level as in (b) (Torrence and Compos 1998).

3.6 Discussion

Most previous tree-ring-based streamflow reconstructions have focused on records from precipitation-sensitive trees (e.g. Case and MacDonald, 2003). This approach cannot be used in the southern Coast Mountains because trees there have complex radial-growth relations with both temperature and precipitation (Laroque and Smith, 1999; Zhang and Hebda, 2004; Larocque and Smith, 2005). These relationships

directly reflect broad-scale hydroclimatic teleconnections that characterize this region (Stahle *et al*., 2006; Ware, 2007).

The hydroclimatic teleconnections shown to influence tree growth in this region are also known to affect streamflow (Moore and Demuth, 2001; Kiffney *et al*., 2002; Gobena and Gan, 2006). I used a temperature-sensitive Engelmann spruce radial growth chronology and a snowpack-sensitive mountain hemlock chronology to reconstruct a proxy record of Chilko River mean summer discharge anomalies.

The dendrohydrological reconstruction, like many others, does not model extreme events well. The reconstruction identifies the low-frequency variations that I attribute to the PDO and that are recorded in the Chilko River instrumental dataset. The influence of both PDO and ENSO systems on the hydroclimate of the southern Coast Mountains is clear from both my SST-discharge correlations and wavelet analysis on the reconstructed Chilko River mean summer discharge. The proxy record is most sensitive to the negative phases of PDO and ENSO, consistent with past work on the hydrologic regimes of BC (Hamlet and Lettenmaier, 1999). Because the model was built for only the months statistically identified as being climatically important for tree growth, I included in the model only the first two months of summer (June and July). In doing so, a relationship between temperature-driven snowmelt and discharge was identified that could then be related to the radial growth index. The 50- and 8-year periodicities revealed in the reconstructed discharge record are related to this temperature signal through the warm phases of the PDO and ENSO.

3.7 Conclusion

Two ring-width chronologies were used to develop a proxy mean summer discharge record for Chilko River for the period 1764-1999. This record is the first to be developed from tree-ring data for a river draining a glacierized watershed in the British Columbia Coast Mountains. It provides insights into streamflow variability over the past 240 years, and it confirms the long-term influence of PDO and ENSO teleconnections on hydroclimatic regimes in the region. It also demonstrate that a carefully selected temperature-sensitive tree-ring chronology can be used in conjunction with a snowpack-sensitive species to provide a proxy record of summer discharge in rivers strongly affected by snow and ice melt.

References

AHCCD. 2009. Adjusted historical Canadian climate data website (http://www.env.gov.bc.ca/rfc/archive/historic.html), last accessed 02/19/2009.

B.C. Environment. 2009. B.C. environment historical snow survey data website (http://www.env.gov.bc.ca/rfc/archive/historic.html), last accessed 02/19/2009.

Beriault, A.L. and Sauchyn, D.J., 2006. Tree-ring reconstructions of streamflow in the Churchill River basin, northern Saskatchewan. Canadian Water Resources Journal 31: 249-262.

Biondi, F. and Waikul, K. 2004. DENDROCLIM2002: A C++ program for statistical calibration of climate signals in tree-ring chronologies. Computers and Geosciences 30: 303-311.

Blown, I. and Church, M. 1985. Catastrophic lake drainage within the Homathko River basin, British Columbia. Canadian Geotechnical Journal 22: 551-563.

Case, R.A. and MacDonald, G.M. 2003. Tree ring reconstructions of streamflow for three Canadian Prairie Rivers. Journal of American Water Resources Association 37: 704-714.

Clague, J.J. and Evans, S.G. 2000. A review of catastrophic drainage of moraine-dammed lakes in British Columbia. Quaternary Science Reviews 19: 1763-1783.

Cook, E.R. and Holmes, R.L. 1986. Guide for computer program ARSTAN. Adapted from Users Manual for Program ARSTAN. In: Tree-Ring Chronologies of Western North America: California, Eastern Oregon, and Northern Great Basin, Holmes, R.L. and Fritts, H.C. University of Arizona, Laboratory of TreeRing Research, Tucson, AZ, pp. 50-65.

D'Arrigo, R., Wiles, G., Jacoby, G., and Villalba, R. 1999. North Pacific sea surface temperatures: past variations inferred from tree rings. Geophysical Research Letters 26: 2757-2760.

Desloges, J.R. and Gilbert, R. 1998. Sedimentation in Chilko Lake: a record of the geomorphic environment on the eastern Coast Mountains of British Columbia, Canada. Geomorphology 25: 75-91.

Ettl, G.J. and Peterson, D.P. 1995. Extreme climate and variation in tree growth: individualistic response in subalpine fir (*Abies lasiocarpa*). Global Change Biology 1: 231-241.

Fleming, S.W. and Clarke, G.K.C. 2002. Autoregressive noise, deserialization, and trend detection and quantification in annual river discharge time series. Canadian Water Resources Journal 27: 335–354.

Fleming, S.W. and Clarke, G.K. 2003. Glacial control of water resource and related environmental responses to climatic warming: empirical analysis using historical streamflow data from northwestern Canada. Canadian Water Resources Journal 28: 69–86.

Fleming, S.W. and Quilty, E.J. 2006. Aquifer responses to El Niño-Southern Oscillation, southwest British Columbia. Ground Water 44: 595–599.

Fleming, S.W., Moore, R.D., and Clarke, G.K.C. 2006. Glacier-mediated streamflow teleconnections to the Arctic oscillation. International Journal of Climatology 26: 619–636.

Fleming, S.W., Whitfield, P.H., Moore, R.D., and Quilty, E.J. 2007. Regime dependent streamflow sensitivities to Pacific climate modes across the Georgia-Puget transboundary ecoregion. Hydrological Processes 21: 3264–3287.

Gedalof, Z. and Smith, D.J. 2001a. Dendroclimatic response of mountain hemlock (*Tsuga mertensiana*) in Pacific North America. Canadian Journal of Forest Research 31: 322-332.

Gedalof, Z. and Smith, D.J. 2001b. Interdecadal climate variability and regime-scale shifts in Pacific North America. Geophysical Research Letters 28: 1515-1518.

Gedalof, Z., Peterson, D.L., and Mantua, N.J. 2004. Columbia River flow and drought since 1750. Journal of the American Water Resources Association 40: 1579-1592.

Gobena, A.K. and Gan, T.Y. 2006. Low-frequency variability in southwestern Canadian stream flow: links with large-scale climate anomalies. International Journal of Climatology 26: 1843-1869.

Grissino-Mayer, H.D. 2001. Evaluating cross-dating accuracy: a manual and tutorial for the computer program COFECHA. Tree-Ring Research 57: 205-221.

Guay, R., Gagnon, R., and Morin, H. 1992. A new automatic and interactive tree-ring measurement system based on a line scan camera. The Forestry Chronicle 38: 138-141.

Hamann, A. and Wang, T. 2005. Models of climatic normals for genecology and climate change studies in British Columbia. Agricultural and Forest Meteorology 128: 211-221.

Hamlet, A.F. and Lettenmaier, D.P. 1999. Columbia River streamflow forecasting based on ENSO and PDO climate signals. Journal of Water Resources Planning and Management 125: 333-341.

Hansen-Bristow, K. 1986. Influence of increasing elevation on growth characteristics at timberline. Canadian Journal of Botany 64: 2517-2523.

Holmes, R.L., Adams, R.K., and Fritts, H.C. 1986. Tree-ring chronologies of western North America: California, eastern Oregon and northern Great Basin, with procedures

used in the chronology development work, including user manuals for computer programs COFECHA and ARSTAN. University of Arizona, Laboratory of Tree-Ring Research, Tucson, AZ, Chronology Series VI.

Hughes, M.K. 2002. Dendrochronology in climatology – the state of the art. Dendrochronology 20: 95-116.

Kershaw, J.A., Clague, J.J., and Evans, S.G. 2005. Geomorphic and sedimentological signature of a two-phase outburst flood from moraine-dammed Queen Bess Lake, British Columbia, Canada. Earth Surface Processes and Landforms 30: 1-25.

Kiffney, P.M., Bull, J.P., and Feller, M.C. 2002. Climatic and hydrologic variability in a coastal watershed of southwestern British Columbia. Journal of the American Water Resources Association 38: 1437-1451.

Klinka, K. and Splechtna, B. 1998. Climate-radial growth relationships in some major tree species of British Columbia. University of British Columbia, Department of Forest Sciences, Extension Series 13.

Larocque, S.J. and Smith, D.J. 2003. Little Ice Age glacial activity in the Mt. Waddington area, British Columbia Coast Mountains, Canada. Canadian Journal of Earth Sciences 40: 1413-1436.

Larocque, S.J. and Smith, D.J. 2005. A dendroclimatological reconstruction of climate since AD 1700 in the Mt. Waddington area, British Columbia Coast Mountains, Canada. Dendrochronologia 22: 93-106.

Laroque, C.P. and Smith, D.J. 1999. Tree-ring analysis of yellow-cedar (*Chamaecyparis nootkatensis*) on Vancouver Island, British Columbia. Canadian Journal of Forest Research 29: 115-123.

Laroque, C.P. and Smith, D.J. 2003. Radial-growth forecasts for five-high elevation conifer species on Vancouver Island, British Columbia. Forest Ecology and Management 183: 313-325.

Luckman, B.H. and Wilson, R.J.S. 2005. Summer temperatures in the Canadian Rockies during the last millennium: a revised record. Climate Dynamics 24: 131-144.

MacDonald, G.M. and Case, R.A. 2005. Variations in the Pacific Decadal Oscillation over the past millennium. Geophysical Research Letters 32: doi:10.1029/2005GL022478, 2005.

Mantua, N.J., and Hare, S.J. 2002. The Pacific Decadal Oscillation. Journal of Oceanography 58: 35-44.

Mantua, N.J., Hare, S.R., Zhang, Y., Wallace, J.M., and Francis, R.C. 1997. A Pacific interdecadal climate oscillation with impacts on salmon production. Bulletin of the American Meteorological Society 78: 1069-1079.

Meko, D.M., Therrell, M.D., Baisan, C.H., and Hughes, M.K. 2001. Sacramento River flow reconstruction to A.D. 869 from tree ring. Journal of the American Water Resources Association 37: 1029-1039.

Melack, J.M., Dozier, J., Goldman, C.R., Greenland, D., Milner, A.M., and Naiman, R.J. 1997. Effects of climate change of inland waters of the Pacific coastal mountains and western great basin of North America. Hydrological Processes 11: 971-992.

Moore, R.D. and Demuth, M.N. 2001. Mass balance and streamflow variability at Place Glacier, Canada, in response to recent climate fluctuations. Hydrological Processes 15: 3473–3486.

Moore, R.D., Fleming, S.W., Menounos, B., Wheate, R., Fountain, A., Stahl, K., Holm, K., and Jakob, M. 2009. Glacier change in western North America: influences on hydrology, geomorphic hazards and water quality. Hydrological Processes 23: 42-61.

Morrison, J., Quick, M.C., and Foreman, M.G.G. 2002. Climate change in the Fraser River watershed: flow and temperature projections. Journal of Hydrology 263: 230-244.

Peterson, D.W. and Peterson, D.L. 2001. Mountain hemlock growth responds to climatic variability at annual and decadal time scales. Ecology 82: 3330-3345.

Peterson, D.W., Peterson, D.L., and Ettl, G.J. 2002. Growth responses of subalpine fir to climactic variability in the Pacific Northwest. Canadian Journal of Forest Research 32: 1503-1517.

Rossi, S., Deslauriers, A., Anfodillo, T., Morin, H., Saracino, A., Motta, R., and Borghetti, M. 2006. Conifers in cold environments synchronize maximum growth rate of tree-ring formation with day length. New Phytologist 170: 301-310.

Schiefer, E., Menounos, B., and Wheate, R. 2007. Recent volume loss of British Columbian glaciers, Canada. Geophysical Research Letters 34: doi:10.1029/2007GL030780, 2007.

Schmidt, W.C. and Lotan, J.E. 1980. Phenology of common forest flora of the Northern Rockies-1928 to 1937. U.S. Department of Agriculture, Forest Service, Intermountain Forest and Range Experiment Station, Research Paper INT-259, 20 pp.

Smith, D.J. and Laroque, C.P. 1998. Mountain hemlock growth dynamics on Vancouver Island. Northwest Science 72: 67-70.

Smith, H.A., Blachut, S.P., and Bengeyfield, B. 1987. Study design for fisheries and hydrology assessment in a glacial watershed in British Columbia In: Regulated Streams: Advances in Ecology. Edited by: Crisp, D.T., Craig, J.F., and Kemper, J.B. Plenum Press, NY, 289-301.

Stahl, K., Moore, D., and Mckendry, I.G. 2006. The role of synoptic-scale circulation in the linkage between large-scale ocean-atmosphere indices and winter surface climate in British Columbia, Canada. International Journal of Climatology 26: 541-560.

Stockton, C.W. and Fritts, H.C. 1973. Long-term reconstruction of water level changes for Lake Athabasca by analysis of tree rings. Water Resources Bulletin 9: 1006-1027.

Stokes, M.A. and Smiley, T.L. 1964. An Introduction to Tree-Ring Dating. University of Chicago Press, Chicago, IL.

Thibeault-Martel, M., Krause, C., Morin, H., and Rossi, S. 2008. Cambial activity and intra-annual xylem formation in roots and stems of *Abies balsamea* and *Picea mariana*. Annals of Botany doi:10.1093/aob/mcn146.

Torrence, C. and Compo, G.C. 1998. A practical guide to wavelet analysis. Bulletin of the American Meteorological Society 79: 61-78.

van Oldenborgh, G.J. and Burgers, G. 2005. Searching for decadal variations in ENSO precipitation teleconnections. Geophysical Research Letters L15701, doi:10.1029/2005GL023110.

Vanlooy, J.A.; and Forster, R.R. 2008. Glacial changes of five southwest British Columbia icefields, Canada, mid-1980s to 1999. Journal of Glaciology 54: 469-486.

VoorTech Consulting. 2008. MeasureJ2X [computer program]. Project J2X, Version 4.1.2. Holderness, NH.

Walker, I.R. and Pellatt, M.G. 2008. Climate change and ecosystem response in the northern Columbia River basin – a paleoenvironmental perspective. Environmental Reviews 16: 113-140.

Wang, J.Y., Whitfield, P.H., and Cannon, A.J. 2006. Influence of Pacific climate patterns on low-flows in British Columbia and Yukon, Canada. Canadian Water Resources Journal 31: 25-40.

Ware, D.M. 2007. A century and a half of change in the climate of the NE Pacific. Fisheries Oceanography 4: 256-277.

Watson, E., and Luckman, B.H. 2005. Tree-ring based records of precipitation and streamflow in the southern Canadian Cordillera. In: Water, Ice, Land, And Life: The Quaternary Interface. Canadian Quaternary Association, University of Manitoba, Winnipeg, MB, Abstract Volume: A103.

Whitfield, P.H. 2001. Linked hydrologic and climate variations in British Columbia and Yukon. Environmental Monitoring and Assessment 67: 217-238.

Wigley, T.M. L., Briffa, K.R., and Jones, P.D. 1984. On the average value of correlated time series, with applications in dendroclimatalogy and hydrometeorology. Journal of Applied Meteorology 23: 201-213.

Wilkie, K.M.K. 2006. Fluvial response to Late Holocene glacier fluctuations in the Nostetuko River valley, southern Coast Mountains, British Columbia. M.Sc. thesis, Simon Fraser University, Burnaby, BC.

Wilson, R.J.S. and Luckman, B.H. 2003. Dendroclimatic reconstruction of maximum summer temperatures in British Columbia. The Holocene 13: 851-861.

WSC. 2009. HYDAT archived hydrometric data. Environment Canada, Water Survey of Canada, Ottawa, ON. www.wsc.ec.gc.ca/hydat/H2O/, last accessed 02/19/2009.

Zhang, Q. and Hebda, R.J. 2004. Variation in radial growth patterns of *Pseudotsuga menziesii* on the central coast of British Columbia, Canada. Canadian Journal of Forest Research 34: 1946-1954

Zhang, Q., Alfaro, R.I., and Hebda, R.J. 1999. Dendroecological studies of tree growth, climate and spruce beetle outbreaks in central British Columbia, Canada. Forest Ecology and Management 121: 215-225.

Chapter Four: Summary and Conclusion

4.1 Summary

I used dendrochronological techniques to study the late Holocene geomorphic and hydrologic history of the west branch of the Nostetuko River in the central British Columbia Coast Mountains. The study took advantage of the 1997 catastrophic drainage of moraine-dammed Queen Bess Lake. The outburst flood from the lake eroded the Holocene sediment fill in the valley below the lake, exposing a series of subfossil forest layers separated by overbank floodplain sediments. The exposures provided a valuable opportunity to date periods of floodplain stability and intervening periods of paraglacial fluvial aggradation. Construction of tree-ring chronologies for the study area also permitted examination of the relationship between radial tree growth and hydroclimate.

I developed living Engelmann spruce and subalpine fir chronologies for the study area and a subalpine fir chronology for the central Coast Mountains (Chapter 2). All chronologies have significant average series intercorrelation values. The Engelmann spruce chronology spans 352 years (1656-2007) and contains 38 series. Due to limited sample depth prior to 1775, the earliest portion of the chronology displays considerable annual variability. The study site subalpine fir chronology spans 279 years (1729-2007) and contains 29 series. The composite regional chronology contains over 250 series and extends the subalpine fir tree-ring record back to 1572 AD.

The living chronologies were used in conjunction with samples taken from subfossilized trees to reconstruct paraglacial valley-fill events over the past 1200 years (Chapter 2). Of the 135 subfossil trees sampled, none exhibited adventitious roots, one of

the most common responses in trees that survive burial. Some trees showed signs of suppressed radial growth, traumatic resin canals, and reaction wood. These periods were found at the end of the ring-width series; as such I interpreted this to indicate that the aggradation event killed the trees. Analysis on the successfully dated subfossil samples revealed six major sediment deposition events that coincide with regional, independently dated glacial advances over the past 1200 years. Valley-wide aggradation during these events is interpreted to result from increased sediment supply from glaciers that advanced into the west fork of the Nostetuko valley.

Dendroclimatological and dendrohydrological techniques were used to reconstruct summer stream discharge of the nearby Chilko River (Chapter 3). An examination of the hydroclimatic parameters correlated to mean summer discharge of the Chilko River, revealed significant correlations with summer temperature and winter snowpack. Response function analysis identified the radial growth of Engelmann spruce from the banks of the west branch of the Nostetuko was found to be positively related to summer temperature. The radial growth of the Oval Glacier mountain hemlock chronology was found to be positively correlated to summer temperatures and negatively correlated to winter snowpack. These relationships allowed for the reconstruction of a proxy record of mean summer discharge of the Chilko River for the period 1762-1999 from tree rings. The reconstructred discharge index was correlated with SST fields and dominate periodicities were extracted using wavelet analysis to confirm the long-term influence of the PDO and ENSO on the hydroclimatic regime of the region.

4.2 Conclusions

My research has shown that proglacial fluvial sediment records can be used to develop a record of climate and glacial activity during the Little Ice Age in the Coast Mountains. I have demonstrated that LIA-related paraglacial aggradation within the west branch of the Nostetuko occurred over a valley-wide spatial scale. By developing a record of six periods of aggradation over the LIA, my research shows that proglacial fluvial sediment systems can be sensitive recorders of climate and glacier change. This technique may be used to develop a more complete, albeit less direct, record of glacial activity than dendroglaciological methods, which rely on dating trees that have been directly impacted by glaciers.

I have also shown that a temperature-sensitive tree-ring chronology can be used in tandem with a snowpack-sensitive tree-ring chronology to provide a proxy record of summer discharge of rivers that are strongly affected by snow and ice melt. In doing so, I have created the first tree-ring based reconstruction of discharge for the British Columbia Coast Mountains. The reconstruction demonstrations that mean summer discharge for the Chilko River and the region have fluctuated significantly over the past 200 years. I have shown that a significant portion of this variability can be attributed to large scale ocean-atmosphere circulation phenomena, such as the PDO and ENSO. This has implications for water resource management, in that managers need to adapt their strategies to account for decadal-scale variation.

Appendix 1 – Ring-width chronology used in this thesis

Appendix 1a: The standard regional subalpine fir chronology developed in this research. Data are shown in decadal format with index values presented to the nearest 0.001. A negative 9999 indicates the end of the series.

Decade	Index value									
1572	367	498	345	632	772	1369	1078	694		
1580	524	526	699	1471	1355	1225	1312	1560	1984	1077
1590	596	812	980	1188	1291	1380	1319	1143	1056	795
1600	921	675	1056	749	933	967	1182	1174	1303	1141
1610	1320	867	972	529	503	863	1229	1111	858	715
1620	995	1458	1364	1239	1248	688	796	1113	811	1294
1630	1445	1077	1405	909	1190	1472	1144	832	1238	963
1640	1092	806	1228	1016	1125	1071	833	756	943	1135
1650	973	1100	1192	949	1327	1185	1069	762	1212	1019
1660	855	980	955	851	781	1131	958	882	773	844
1670	1118	764	1060	1104	923	1069	738	1117	877	788
1680	1004	908	1186	1071	1155	987	911	1149	1045	1130
1690	1109	956	1016	926	547	914	927	484	845	688
1700	864	574	643	557	751	884	642	959	957	997
1710	1223	988	1259	1406	1275	906	1143	1123	1115	1048
1720	1081	1314	1055	994	850	887	1140	1228	1161	1106
1730	898	943	963	1012	982	993	1038	1240	1058	1104
1740	921	989	948	934	785	907	845	1020	1074	1047
1750	1032	829	738	973	907	873	1145	1088	1072	941
1760	970	948	890	1000	1115	908	1136	1023	885	1089
1770	992	1039	854	1025	1131	809	1020	1220	1003	854
1780	1050	963	864	1090	965	971	939	937	991	991
1790	947	931	1127	1022	1130	1160	1135	978	1106	1024
1800	1088	1029	985	1141	1114	1230	1064	1113	1029	1013
1810	895	1053	907	900	940	839	1024	1084	1043	859
1820	1043	900	1001	1025	949	1162	963	880	1006	985
1830	1044	1057	996	1045	1207	1088	937	1084	904	1276
1840	969	892	988	1044	975	831	950	796	1054	892
1850	888	1033	1049	1016	950	1158	979	1035	966	988
1860	912	923	887	1156	799	1131	768	796	940	967
1870	920	938	897	1034	1015	1153	784	971	857	969
1880	948	919	877	925	914	973	947	958	948	852
1890	927	1003	910	821	946	872	909	891	930	865
1900	949	1075	1200	1222	1226	1165	1174	1206	1206	959
1910	1033	1067	1060	1044	1113	1253	834	1107	1153	982
1920	1090	891	1086	1051	928	824	1136	1158	1041	1001
1930	1142	1013	954	1044	894	1013	950	1135	1135	928
1940	1002	1241	1214	916	1219	1114	906	988	1222	1086
1950	1079	944	915	875	846	1058	882	875	1204	878
1960	1073	965	852	947	903	1219	1000	1111	952	889
1970	1087	872	808	886	699	994	742	1095	1018	883

1980	877	1092	945	780	1059	1064	850	913	938	765
1990	1115	730	1208	922	1097	1080	1054	1042	1215	1024
2000	1233	1252	1193	1133	1154	956	1155	968	-9999	

Appendix 1b: The Engelmann spruce residual chronology used in this research. Data are shown in decadal format with index values presented to the nearest 0.001. A negative 9999 indicates the end of the series.

Decade	Index value									
1659	826									
1660	1282	1078	1124	1218	689	890	737	1170	819	891
1670	830	1184	1140	1366	1194	1173	1027	1252	1234	1264
1680	682	812	987	1259	785	1036	961	755	637	784
1690	789	766	833	861	773	725	884	886	821	984
1700	930	1048	917	885	892	1045	1002	1116	1362	1125
1710	1103	1170	1038	1116	948	668	963	1107	1134	1001
1720	758	1074	1162	945	1081	938	1159	1431	915	971
1730	1204	972	994	908	864	719	1026	958	873	967
1740	962	1021	884	837	1034	1004	972	976	1042	888
1750	1109	878	1070	1049	1154	1109	978	748	1009	949
1760	976	1206	974	1075	993	869	976	1016	1022	1009
1770	886	1155	783	1106	879	919	1010	1143	802	842
1780	822	949	927	879	995	955	955	922	855	1017
1790	1027	994	1181	893	1003	990	942	1062	1098	854
1800	991	969	936	956	1097	1015	949	985	1049	992
1810	1058	1087	935	866	905	1005	1122	1021	1035	1037
1820	1032	1042	974	995	913	1040	965	969	1013	868
1830	1002	919	1079	1070	1080	801	897	1015	862	1047
1840	877	904	1089	992	920	1053	908	1071	1005	944
1850	1107	997	940	985	933	1056	933	1084	916	962
1860	953	990	1091	1139	896	988	975	971	1050	991
1870	895	975	1084	947	1024	971	768	931	1052	1064
1880	1068	929	1068	936	963	923	1111	1111	1032	957
1890	974	1074	870	881	1085	911	1056	959	988	881
1900	1090	991	1104	1170	1068	954	848	1161	1098	894
1910	862	927	906	900	1098	1051	916	946	987	884
1920	1030	903	1138	916	889	935	877	962	942	898
1930	1031	862	869	1063	972	1083	1009	1198	1218	827
1940	1103	1072	1088	880	1113	1191	1000	973	1205	1075
1950	1232	1009	1072	1079	997	1020	1030	980	1227	866
1960	1154	1117	862	1184	956	1141	773	1162	1056	1183
1970	945	727	953	824	839	1076	853	1077	979	819
1980	902	979	945	907	928	939	844	1007	898	1030
1990	1000	897	1091	834	983	1063	931	950	1085	1097
2000	1209	1132	1102	1054	1010	881	1070	844	-9999	

Appendix 1c: The mountain hemlock residual chronology used in this research. Data are presented in decadal format with index values shown to the nearest 0.001. A negative 9999 indicates the end of the series.

Decade	Index value									
1765	1309	1056	686	915	910					
1770	1532	996	566	1241	372	932	1436	1386	795	498
1780	1181	881	995	1082	546	899	989	851	1054	941
1790	735	961	1357	1087	1103	1105	830	918	1117	946
1800	1152	897	961	989	1133	1047	826	844	886	904
1810	774	788	991	953	1075	1042	1039	894	1055	704
1820	853	902	1158	1026	902	948	1054	1014	946	1185
1830	1068	884	1092	1154	1235	1197	788	1158	854	1208
1840	859	1005	1188	1291	1136	723	906	929	1350	740
1850	858	1060	1055	1086	904	1130	858	1072	963	997
1860	882	1120	940	1086	806	1009	697	912	1201	901
1870	859	840	832	1215	1097	936	752	1123	1003	883
1880	829	862	918	933	986	1141	754	718	997	1107
1890	1175	1001	949	668	726	895	810	1027	1108	886
1900	1050	950	1142	995	1189	1003	893	1013	1066	895
1910	900	642	724	822	1093	1385	709	961	1127	882
1920	1008	898	1087	1114	1000	800	1369	970	1004	1086
1930	1080	960	822	961	1239	1064	908	1131	1156	1026
1940	1108	1357	1186	782	1193	1060	895	1061	1049	1029
1950	981	1046	731	1001	1004	1085	985	1009	1080	1010
1960	1079	1148	998	1129	995	1266	987	1028	1024	690
1970	979	948	822	1104	710	1106	776	1371	988	1008
1980	1084	1068	827	1001	1319	952	794	1114	975	882
1990	1000	558	1188	1167	1264	908	886	989	1249	904
2000	-9999									

Appendix 2 – Subfossil sample data

Appendix 2a: Field and laboratory data on subfossil trees sampled along the west branch of the Nosetuko River.

Sample no.	Species[a]	Site	Height[b]	Series length[c]
1	wbp	E	2	67
2		E	2	P
3	wbp	E	2	72
4	wbp	E	1.85	55
5		E	1.85	P
6		E	4	P
7	saf	E	2	49
8		E	3.5	P
9	saf	E	2.5	53
10	wbp	E	2.5	25
11		E	3.5	P
12	wbp	E	3.8	76
13		E	3.5	P
14		E	3	P
15		E	3	P
16	saf	E	3.75	118
17		E	4	P
18		E	4.5	P
19		E	3	P
20	wbp	E	2	30
21		E	2	P
22		E	0.75	P
23	wbp	E		173
24	wbp	E	0.5	48
25		E	0.75	p
26		E	2	p
27		E	0.75	p
28		E	1	p
29	wbp	E	0.75	96
30		E	4	p
31		D	4	p
32	wbp	D	1.5	134
33		D	2.5	p
34	saf	D	0.5	150
35		D	2	p
36		D	2.5	p
37		D	2.25	p
38	saf	D	1.5	152
39		D	1.25	p
40		D	1.25	p
41		D	1.25	p

42		F	2	p
43		F	1.25	p
44	saf	F	2	151
45	saf	F	2	136
46	wbp	F	2.2	132
47		F	0	p
48	saf	F	1.5	p
49	saf	F	1	50
50		F	0.25	p
51		F	0.25	p
52	wbp	H	1	123
53		H	0.25	p
54		H	0.1	p
55	wbp	H	0.1	156
56		H	0	p
57		H	0.5	p
58		H	0	p
59		H	0.2	p
60		H	0.2	p
61	saf	H		245
62		H	2.5	p
63	saf	H		p
64	saf	H	0.5	284
65	es	H	0	77
66		H	0.1	p
67		H	0.1	p
68		H	0	p
69	saf	H	1	220
70		H	0.25	p
71	saf	H	0.25	138
72		H	0.1	p
73	saf	H	0	137
74		H	3.5	p
75		H	1.25	p
76		H	3.5	p
77		H	2	p
78	saf	H	0.1	155
79	wbp	H	0.75	107
80		H	0.8	p
81		H	2.5	p
82		H	0.5	p
83		H	0.5	p
84	wbp	H		211
85		H	0.75	p
86		H	0.25	p
87		H	0.25	p
88	wbp	H	0	88
89	es	H	2.5	161
90	es	H	2.5	165
91	saf	H	0.5	110

92	es	H	0.5	134
93	saf	H	2.5	96
94	saf	H	2.5	58
95		H	0	173
96		H	0	p
97		H	0.75	p
98		H	0.25	p
99	es	H	1.25	55
100	wbp	H	1.75	60
101	saf	H	1.5	37
102		H	1.25	p
103		I	1.5	p
104	saf	I	1.5	70
105	es	I	1.5	120
106	saf	I	1.75	84
107		I	1.5	p
108	saf	I	0	79
109		I	1.5	p
110		I	0	p
111	saf	I	0	54
112		I	1.5	p
113		I	1.5	p
114	saf	I	0.25	64
115		I	0.25	p
116		I	0.1	p
117		I	0.25	p
118		I	0.25	p
119	saf	I	0.2	77
120		I	0.2	p
121	saf	I	0.5	132
122		K	-0.1	p
123		K	-0.1	p
124		K	0	p
125		K	-0.1	p
126	es	K	-0.1	92
127	saf	J	0	86
128		J	0	p
129		J	0	p
130	es	J	0.5	42
131		J	0	p
132	saf	J	0	78
133		C	3	p
134	saf	C	3	128
135	saf	E	3.5	42

[a] saf = subalpine fir; es = Engelmann spruce; wbp = whitebark pine.

[b] height measured above water level.

[c] p = sample was too problematic for dendrochronological analysis.

Appendix 3 – Summer temperature reconstruction

Dendroclimatological relationships

In Chapter 3, the radial growth of Engelmann spruce was identified as being significantly correlated to summer temperatures (Fig. 3.5). This signal is evident whether minimum, maximum, or mean monthly temperature is used, but the strongest response and correlation coefficients are found with mean temperature. This relationship is stable through time – the scatterplot of paired tree-ring index and mean temperature data shows a consistent linear relationship ($r^2 = 0.2258$) (Appendix 3a). The stability of the correlation between June-July temperature and annual radial growth through time was further analyzed by calculating block correlations of 30 years duration with an overlap of 15 years. All 30-year blocks are significantly correlated, leading me to conclude that the relationship is stable through time (Appendix 3b).

Dendroclimatological reconstructions

Linear regression was used to model the relationship between summer temperature and radial tree-ring growth for a calibration period from 1968 to 2005 (Appendix 3c). The model captures low-frequency variations in temperature successfully for both the calibration and verification (1930-1967) periods. It accounts for 61% of the variability in the verification data at the 99% confidence level (Appendix 3d).

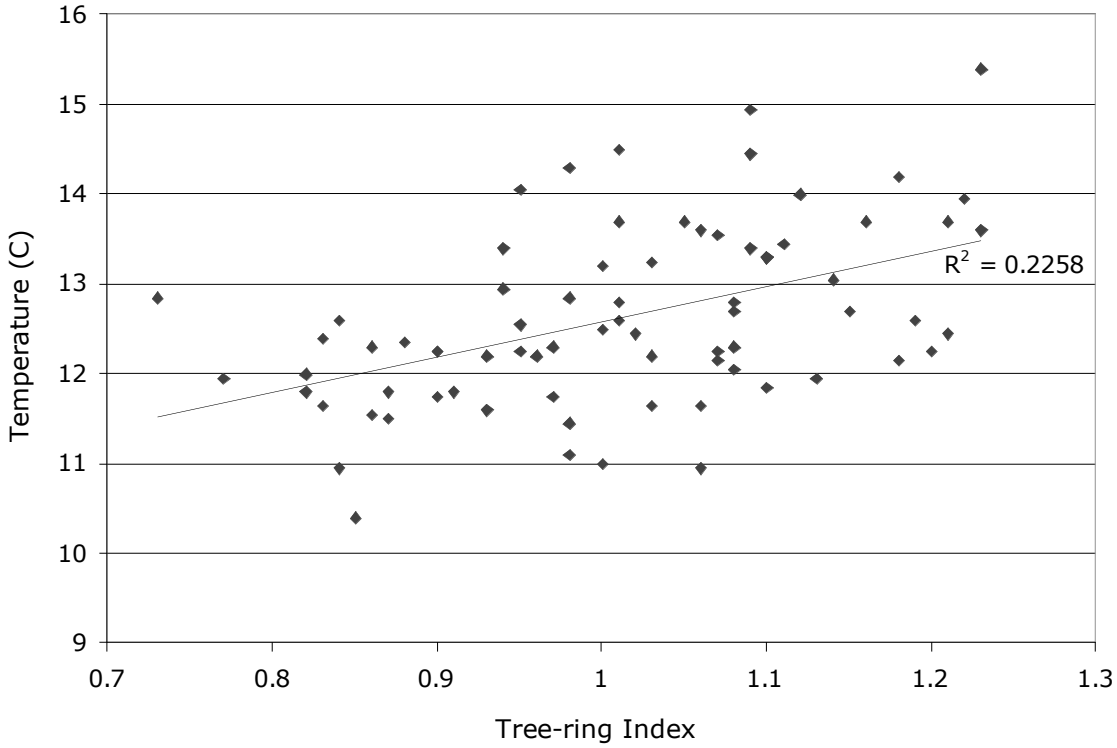

Appendix 3a: Scatterplot showing the relation between radial growth of Engelmann spruce and average summer (June-July) temperature at Tatlayoko Lake.

Appendix 3b: Block correlations calculated for each modeled variable.

Variable	Start year	End year	Correlation
Mean summer temperature	1930	1959	0.615 [a]
	1945	1974	0.541 [a]
	1959	1988	0.478 [a]
	1974	2003	0.467 [a]

[a] Significant at the 99% confidence level..

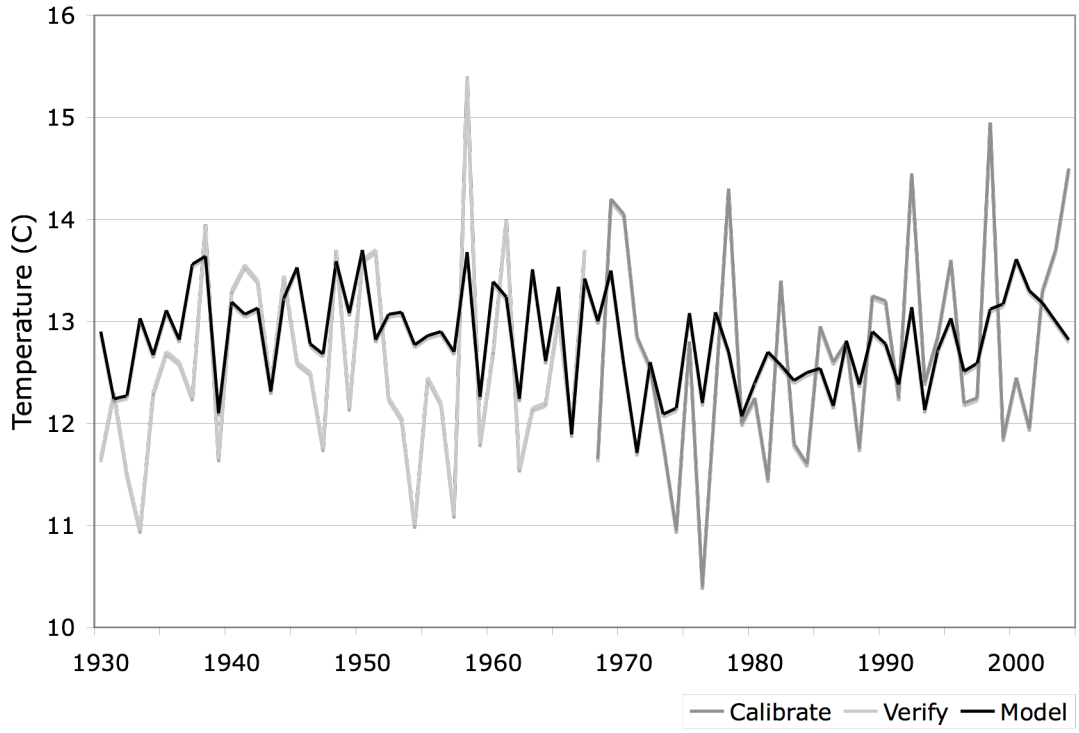

Appendix 3c: Summer temperature model based on a linear relationship with the radial growth of Engelmann spruce.

Appendix 3d: Model summaries for mean summer temperature and stream flow reconstructions using Engelmann spruce ring width as the predictor.

	Model	Calibration correlation	Verification correlation	Total correlation
Mean summer temperature	y = 8.850 + 3.933x	0.415	0.611	0.474

All correlations are significant at the 99% confidence level..

Based on the strength of this relationship, I calculated a mean summer temperature anomaly record for the period 1775-2005 (Appendix 3e). The proxy record indicates that temperatures at the site have considerable year-to-year variability. Cool summers occurred throughout the period; the coolest summers were in 1835, 1876, 1966, and 1974. Relatively warm summers occurred in 1792 and 1958, and the interval 1930-1969 is the most sustained period of warm summers during the past two centuries. The reconstruction displays little low-frequency periodicity before 1900. Beginning in the 20th century, however, multi-decadal intervals of cool summers (1905-1929, 1970-1988) alternate with warm intervals of similar length (1930-1969, 1989-2006). A model of summer temperature was generated from the Engelmann spruce chronology, but the explained variance is low and does not provide new insight into past climate.

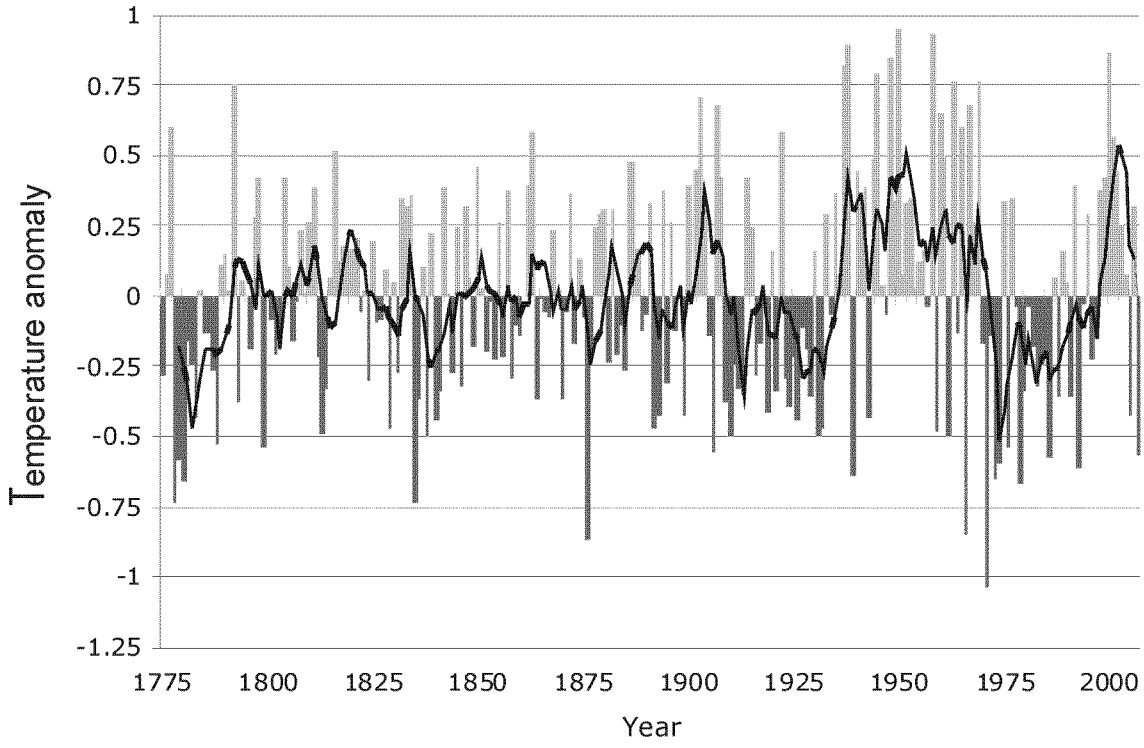

Appendix 3e: Reconstructed summer temperature anomalies based on a linear model developed from the radial growth of Engelmann spruce.